Strata, structures and enduring enigmas: A 125th Anniversary appraisal of Colorado Springs geology

Chapter · October 2013

DOI: 10.1130/2013.0033(13)

3 authors:

Christine S Siddoway
Colorado College

Paul M. Myrow
Colorado College

Elisa Fitz Diaz
Universidad Nacional Autónoma de México

Field Guides

Strata, structures, and enduring enigmas: A 125th Anniversary appraisal of Colorado Springs geology

Christine Siddoway, Paul Myrow and Elisa Fitz-Díaz

Field Guides 2013;33;331-356
doi: 10.1130/2013.0033(13)

Notes

The Geological Society of America
Field Guide 33
2013

Strata, structures, and enduring enigmas: A 125th Anniversary appraisal of Colorado Springs geology

Christine Siddoway*
Paul Myrow
Department of Geology, The Colorado College, Colorado Springs, Colorado 80903, USA

Elisa Fitz-Díaz*
Department of Earth & Environmental Sciences, The University of Michigan, Ann Arbor, Michigan 48109, USA

ABSTRACT

Although the southern Front Range in Colorado Springs and Manitou Springs contains a near-complete record of Rocky Mountains geological evolution from Proterozoic to Present, there nevertheless are persistent geological problems that have eluded understanding for as much as 125 years. In keeping with the 2013 GSA Annual Meeting theme, "Celebrating Advances in Geoscience," this field trip visits long-known elements of Front Range geology that merit reexamination within the context of new paleoenvironmental and geochronology data. Of note are: (1) the Great Unconformity and its chemically weathered substrate that correspond to a time of profound changes in global ocean chemistry; (2) lower Paleozoic strata that record sea-level fluctuations, attributable in part to regional tectonism; (3) an array of granite-hosted sandstone dikes, for which a new emplacement model is proposed; and (4) the Front Range monocline at Garden of the Gods Park, examined from the standpoint of its temporal evolution, newly bracketed by results of $^{40}Ar/^{39}Ar$ age analysis of illite generated by shear upon bedding-parallel faults.

FIELD TRIP OVERVIEW

This trip begins with an examination of sedimentological records of environmental change within the Paleozoic stratigraphic succession and review of the configuration and timing of major faults associated with the Front Range monocline in Colorado Springs (Fig. 1). It then examines massive sandstone and granite-hosted clastic dikes that are distributed along the Ute Pass fault, structures that have eluded understanding for more than a century. The third realm of study is the structural geology and fault geochronology of Garden of the Gods, with presentation of new isotope data bearing on the time of formation of the Front Range monocline. Two field stops provide participants with vantage points from which to appreciate the scale and extent of the Front Range stratigraphic succession and structures, while close examination of rock exposures is afforded by four roadside stops and three short hikes, including one at the Garden of the Gods Park. Two of the hikes involve off-trail ascent of steep and rough

*csiddoway@coloradocollege.edu; present address, Fitz-Diaz—Instituto de Geología, UNAM, Av. Universidad #3000, C.U., Coyoacán, Mexico, D.F. 04510.

Siddoway, C., Myrow, P., and Fitz-Díaz, E., 2013, Strata, structures, and enduring enigmas: A 125th Anniversary appraisal of Colorado Springs geology, *in* Abbott, L.D., and Hancock, G.S., eds., Classic Concepts and New Directions: Exploring 125 Years of GSA Discoveries in the Rocky Mountain Region: Geological Society of America Field Guide 33, p. 331–356, doi:10.1130/2013.0033(13). For permission to copy, contact editing@geosociety.org.

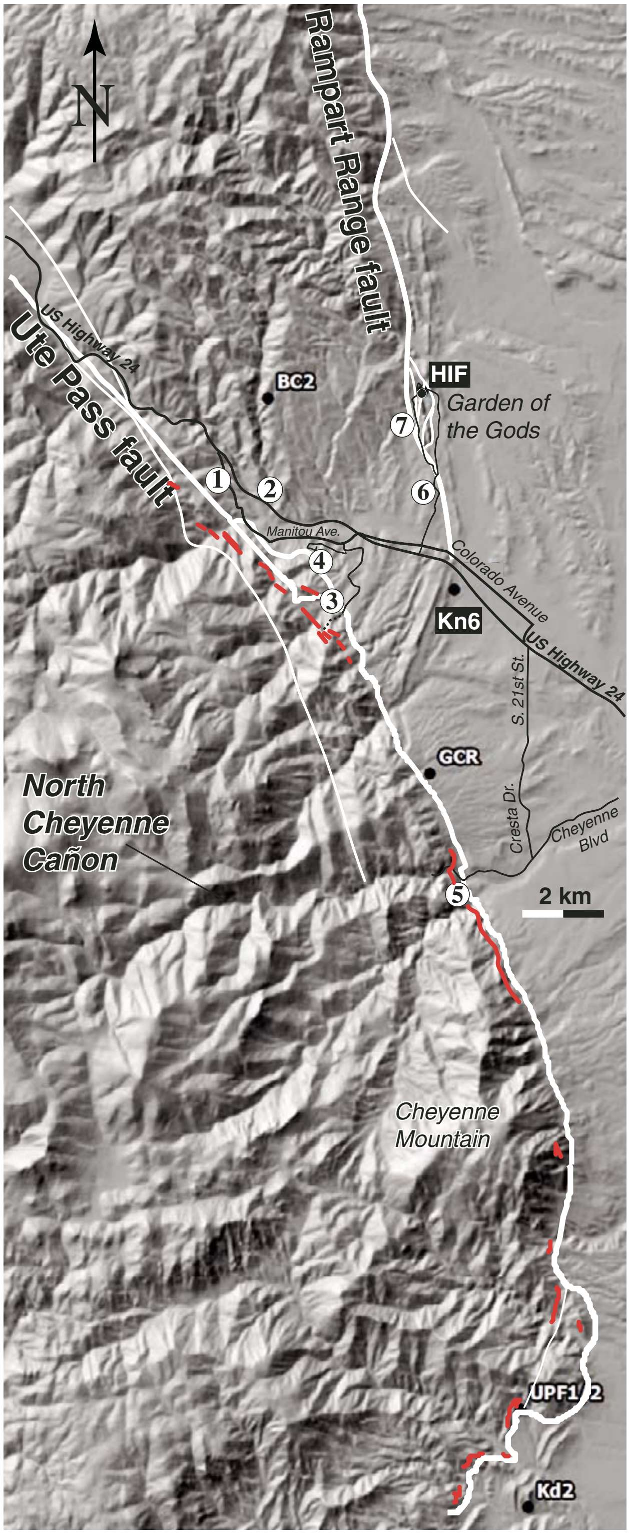

Figure 1. Digital elevation model and location map of part of the southern Front Range near Colorado Springs and Manitou Springs, Colorado. Circled numbers correspond to field trip stops. The traces of the Ute Pass and Rampart Range faults are indicated (white), together with locations of tabular sandstone bodies and sandstone dikes (red) and sample locations for fault gouge geochronology study (ID labels).

terrain, if full access to key relationships is to be achieved. Street directions are given to field stops because the entirety of the trip is within the area of urban development.

In keeping with the theme, "Celebrating Advances in Geoscience," of the 125th Anniversary meeting of the GSA this year, the field trip examines time-honored relationships in a contemporary context, and reports progress in the resolution of enduring geological problems in the Colorado Springs area. The stops were chosen to stimulate discussions about the temporal evolution and geological development of: (1) the Great Unconformity, (2) records of paleoenvironmental transition in lower Paleozoic strata, including glauconite-rich tidal sand waves and karst horizons, (3) a regionally extensive sandstone dike array hosted by Proterozoic granite and gneiss, and (4) the Front Range monocline, based on subsidiary structures in the steep limb of the fold. Notably, the field trip's presentation of new constraints on the timing and mode of emplacement of the clastic dike array coincides with the 120th anniversary of an early GSA Bulletin paper that connotes the onset of geological inquiry in the area. Whitman Cross read his paper "Intrusive Sandstone Dikes in Granite" before the Geological Society of America in 1893.

INTRODUCTION

The southern Front Range in Colorado Springs and Manitou Springs (Fig. 1) offers an expansive record of Rocky Mountains evolution contained within rocks of Proterozoic to Recent age. The Phanerozoic succession is nearly complete, with only the Silurian Period not represented. Sedimentary rocks were the subject of early field investigations reported in initial issues of the Geological Society of America Bulletin (e.g., Cross, 1894; Crosby, 1897), and they provide key records of the Pennsylvanian Ancestral Rocky Mountains orogeny (Suttner et al., 1984; Sweet and Soreghan, 2010) and Cretaceous–Tertiary Laramide orogeny (Kluth and Nelson, 1988; Raynolds, 2002). Existing field guides that review the geology and tectonic evolution of the region include Noblett et al. (1987), Luiszer (1999), Leonard et al. (2002), Milito (2010), Weissenburger et al. (2010), Ross et al. (2010), and Noblett (2011).

The aim of this field trip is to examine advances in understanding of persistent geological problems in the Colorado Springs area. The Great Unconformity is of heightened contemporary interest because of new insights into the global significance of the feature and the consequences of the effects of deep, intense chemical weathering upon the underlying bedrock. Core stones and kaolinitized feldspars in 1.08 Ga Pikes Peak Granite indicate a chemically mature regolith that provided a primary sediment source for the basal Cambrian Sawatch Sandstone, and may have contributed to the profound global shift in ocean chemistry that is linked to the appearance of multicellular life in strata overlying the Great Unconformity worldwide (Peters and Gaines, 2012). Evidence of multicellular life, and of marine incursion, comes from *Teichichnus* and *Paleophycus* burrows in Sawatch Sandstone. The appearance of glauconitic tidal dune deposits

(Myrow, 1998) due to amplification of tidal currents suggests the influence of the geometry of the transgressed landscape upon rising relative sea level and local ocean chemistry at this locality. Stratigraphic revision of Cambrian and Ordovician strata will be outlined, as well as evidence for early Ordovician regional uplift. Deposition of Ordovician through Mississippian carbonate units, with component disconformities, was followed by a significant drop in sea level, recorded by paleokarst breccia at the top of the Mississippian Hardscrabble Limestone. This paleokarst and associated unconformity surface mark a sharp stratigraphic transition from Paleozoic carbonate strata to siliciclastic rocks of the Fountain Formation, associated with onset of the Ancestral Rockies orogeny.

One of the most vexing geological issues to be examined on this trip is the origin and time of emplacement of granite- and gneiss-hosted sandstone along the Ute Pass fault (Kost, 1984; Keller et al., 2005; Temple et al., 2007; Dulin and Elmore, 2013; Freedman et al., 2012). The sandstone dikes and tabular bodies attracted the notice of early geologists in the Front Range (Cross, 1894; Crosby, 1897) and abroad (Journal of the Geological Society of Japan, 1893, in Japanese), but for more than a century there has been poor means to establish the time of sandstone emplacement with certainty because the dikes consist dominantly of quartz, are devoid of fossils, were emplaced within Proterozoic crystalline rock, and are of uncertain provenance. Detrital zircon geochronology (summarized in this guide) and rock magnetic characteristics, including anisotropy of magnetic susceptibility (Freedman et al., 2012), now constrain both age and emplacement mechanism.

An underappreciated challenge in study of the Laramide orogeny is the determination of the precise time of development of specific faults and monoclines. We employed sophisticated methods of mineral separation and $^{40}Ar/^{39}Ar$ illite age analysis of fault gouge (e.g., van der Pluijm et al., 2001, 2006; Haines and van der Pluijm, 2008) to address the underappreciated question of the precise timing of Laramide structural development, obtaining ages that may be compared to the refined lithostratigraphy of synorogenic sediments in Laramide basins (e.g., Obradovich, 2002). The field trip provides context for these new results at Garden of the Gods Park, within the steep limb of the Front Range monocline. The Garden provides an arrested view of the processes of fault linkage and straightening upon segmented, top-to-west reverse faults that developed to accommodate a zone of intensified strain in the footwall of a curved segment of the Rampart Range fault.

STRATA, STRUCTURES, AND ENDURING ENIGMAS

The Great Unconformity and Lower Paleozoic Strata

In this sector of the Front Range, Upper Cambrian rocks rest nonconformably on 1.75-Ga-old metamorphic rocks of the Central Front Range arc sequence (Fisher and Fisher, 2004) and younger plutonic rocks including Pikes Peak Granite (1080 Ma, Smith et al., 1999; Unruh et al., 1995). An anomalously thin lower member of the Sawatch Formation rests directly on the Pikes Peak Granite (Fig. 2; Stop 1). Myrow (1998; Fig. 2) summarized the sedimentology of the lower and middle members of the Sawatch Formation at this locality, and Myrow et al. (2003) provided an overview of lower Paleozoic stratigraphy and depositional history across the state of Colorado. The description and interpretations in this guide are condensed from those sources.

Cambrian Sawatch Formation

Lower Sawatch description. The basal Sawatch Formation at field trip Stop 1 (Fig. 2) consists of 4.0–4.5 m of white-weathering, thin- to medium-bedded (5–20-cm-thick), coarse, very coarse, and pebbly quartz arenite with <5% feldspar (Lewis, 1965). The nonconformity is remarkably flat at the outcrop scale, except where several of the large 0.5–3-m-diameter corestones (quasi-spherical weathering features) in the underlying granite project up to 40 cm above the nonconformity surface into the overlying lower Sawatch. Stratification in the Sawatch clearly abuts against the corestone, indicating that these are Cambrian or older weathering structures.

The lower 2.3 m of the lower Sawatch is parallel laminated with widely spaced, small-scale (<8-cm-thick), trough cross-stratified beds, and thin pebble lags. Clasts of granite and feldspar are found above the basal contact. There are well-preserved polygonal cracks filled with pebbly sandstone at 0.95 m in the section. Above 2.3 m, beds are dominantly bioturbated and separated by partially dispersed (bioturbated) pebble lags with sandstone intraclasts up to 10 cm in diameter. The upper 60 cm of the lower Sawatch is a distinctive white weathering, bioturbated pebbly coarse sandstone bed with abundant burrows, including *Teichichnus* and lined burrows of cf. *Paleophycus*. The uppermost 10 cm of the bed consists of a hematite-coated lag with abundant quartz pebbles, large intraclasts of quartz sandstone, as well as pyritic steinkerns and pyrite-replaced and silicified cephalopod, gastropod, trilobite, and brachiopod shells. In thin section, small, mm-diameter burrows project inwards radially around rounded (<1-cm-diameter) intraclasts of mudstone that must have been firm enough shortly after deposition to withstand transport and rounding. Directly overlying the lag surface are glauconite-rich deposits of the middle Sawatch member.

Lower Sawatch interpretation. The lower member of the Sawatch contains no evidence of multi-cycle grains (e.g., with rounded overgrowths; Lewis, 1965), yet it is compositionally mature, even in poorly sorted pebbly sandstone beds. These observations suggest that the underlying basement was subjected to intense chemical weathering that produced a highly compositionally mature regolith that was a primary sediment source for the Sawatch. Similar processes are envisioned for the Great Unconformity, and directly overlying strata, worldwide (Peters and Gaines, 2012). Erosion of the regolith was uniform through a deeply weathered zone, except where resistant corestones projected up into the weathered profile. Paleoenvironments for the lowermost Sawatch are difficult to interpret because of the

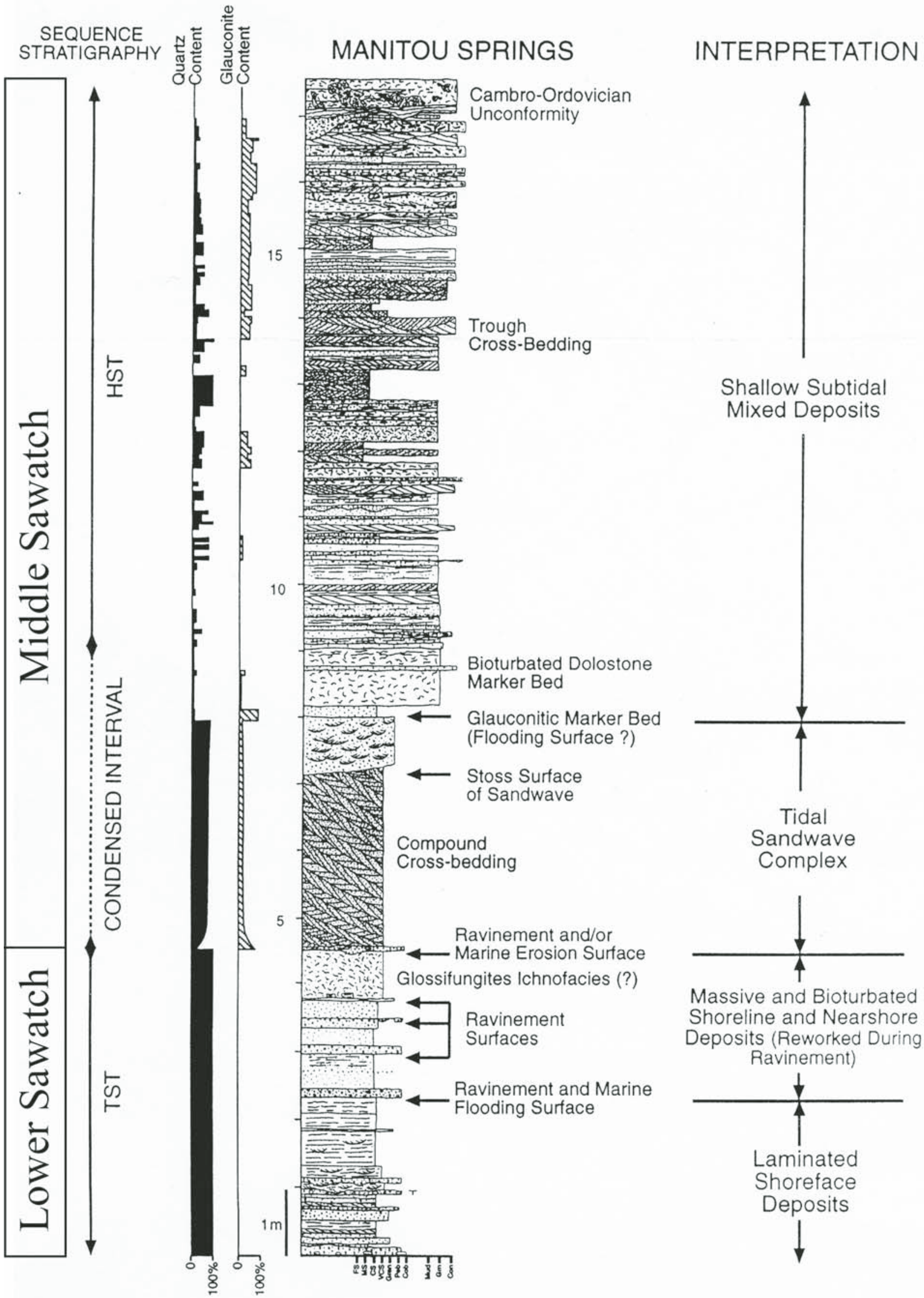

Figure 2. Lithostratigraphy of Cambrian deposits of Colorado (modified from Gerhard, 1972).

paucity of diagnostic sedimentary structures. The strata up to 2.3 m do not contain structures diagnostic of braided stream deposition, such as lenticular beds or abundant dune-scale trough cross-stratified beds. The rarity of cross-strata is unusual because dunes are common in sediment of this grain size in most fluvial and marginal marine environments. Abundant horizontal stratification and the presence of desiccation cracks at 0.9 m suggest that these may be foreshore (beach) deposits, or extremely shallow fluvial strata deposited in either very shallow water or in hyperconcentrated flows, which would have limited the development of dune-scale bedforms.

The presence of bioturbation fabrics and burrows, such as *Teichichnus*, above 2.3 m indicates a marine paleoenvironment. The stratigraphic position of the first significant marine flooding surface may be at 2.3 m, at the sudden shift from laminated beds to massive bioturbated beds. This surface and most of the overlying pebble lags represent potential ravinement or marine erosion surfaces. Intervening sandstone beds represent redistributed sediment, thin remnants of any number of possible nearshore and shoreline subenvironments. Such a stratigraphic record would be expected from small changes in relative sea level in a cratonic setting with low sediment input, low accommodation space, and low equilibrium bottom slopes (Myrow, 1998; Myrow et al., 2003; Runkel et al., 2007, 2008). We envision the Sawatch to record transgressive reworking of a landscape lacking significant fluvial systems, and consisting instead of a low-relief bedrock surface mantled with a thick regolith.

The uppermost bed of the lower member may contain an assemblage of trace fossils of the *Glossifungites* ichnofacies, which form above omission surfaces in firm but unlithified marine shoreline deposits (Frey and Seilacher, 1980; Pemberton and Frey, 1985). Although *Teichichnus* and cf. *Paleophycus* are not restricted to the *Glossifungites* ichnofacies, the sandstone intraclasts and burrows in the small mudstone intraclasts are consistent with firmground conditions. Myrow (1998) interpreted the uppermost lag as a major ravinement surface formed by tidal currents (i.e., Allen and Posamentier, 1993).

The facies transition to overlying glauconitic and dolomitic dune deposits of the middle member is very sharp. Such transitions are common across ravinement surfaces, particularly when zones of active erosion are wide (onshore to offshore) so that more distal marine sediment is deposited above the ravinement surface (Swift, 1968; Allen and Posamentier, 1993; Reynaud et al., 1999; Cattaneo and Steel, 2003). The Sawatch lag is interpreted to represent part of a condensed deposit in which slow sedimentation rates and unusual geochemical conditions produced pyritic, silicic, and hematitic replacement and coatings of grains.

Middle Sawatch description. The middle Sawatch member consists of 13 m of dolostone, sandy dolostone, and dolomitic sandstone with variable amounts of glauconite (Fig. 2). Its base is marked by the appearance of thick, coarse-grained, compound cross-bed sets that rest directly on the uppermost lag of the lower member. The cross-stratification consists primarily of dolomite-cemented detrital grains of quartz, dolomite, glauconite, and white-weathering inarticulate brachiopod shell fragments. Individual cross-bed sets range up to 3.5 m in thickness, and consist of complete or near-complete form sets (preserved dune geometries). Thick co-sets, between 3 and 5 m in thickness, consist of 2–3 stacked to shingled sets of cross-strata. The compound cross-bedded form sets contain nearly symmetrical cross-sectional shapes and low stoss (3°–8°) and foreset (10°–15°) dips. Foreset dip directions are fairly consistent from NNE to NW (Fig. 3). Small-scale cross bedding consists of cm- to dm-scale sets that record the migration of smaller secondary dunes across the larger dunes. These show bimodal to slightly polymodal paleocurrent orientations (Fig. 3).

The rest of the upper member consists of thin- to medium-bedded, complexly mixed, siliciclastic and carbonate strata that range from nearly pure dolomudstone to quartz arenite. Sandstone beds are medium to coarse grained, <6 cm to 50 cm in thickness, and have planar lamination and trough cross bedding. Bioturbation is common in the middle part of the middle member and burrows include *Planolites*, *Chondrites*, *Curvolithus*, and

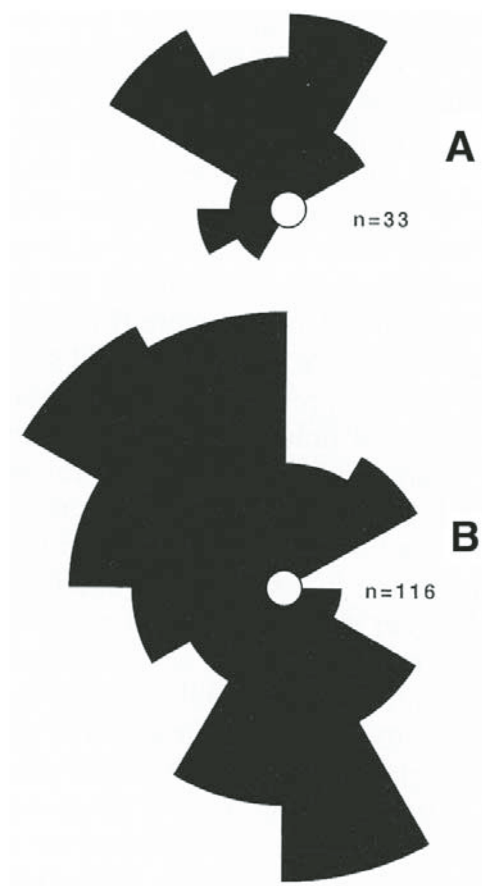

Figure 3. (A) Equal-area rose diagram showing dip directions of large-scale foresets of tidal dunes. (B) Rose diagram showing dip directions of superimposed small-scale cross beds. North toward top of page.

possible *Thalassinoides horizontalis* (Myrow, 1995). There is a decrease in bioturbation and an increase in the abundance of trough cross-stratified and intraclast-rich beds toward the top of the member.

A distinctive, 50–100-cm-thick, competent, red, coarse dolostone unit marks a disconformity contact between the middle Sawatch and overlying Manitou Formation. This highly recrystallized coarse dolostone bed has a sharp erosional lower surface (~40 cm of relief) and a complex internal microstratigraphy that includes karstic cavities with collapse breccia and carbonate cement-filled vugs. Conodonts from this bed are from the Lower Ordovician *Rossodus manitouensis* Zone. The immediately overlying carbonate beds contain conodonts of the subsequent low-diversity interval (i.e., the base of Fauna D of Ethington and Clark, 1981). Two closely spaced sequence boundaries therefore bracket this bed. The basal surface is the mid-*Rossodus* Unconformity (Myrow et al., 2003), which along the Front Range of Colorado represents a considerable Cambrian–Ordovician hiatus.

Middle Sawatch interpretation. The stratigraphic shift to the glauconitic tidal dune deposits of the lowermost middle member represents a significant paleoenvironmental change across a tidal ravinement surface. Modern large tidal dunes in many locations globally rest directly on ravinement surfaces produced during Holocene transgression (e.g., Davis et al., 1993). Marine transgression has generally been implicated in the formation of such dune complexes (e.g., Hine, 1977) and in deposition of glauconite (Brasier, 1980; Odin and Fullagar, 1988). We interpret the dune deposits of the Sawatch to be reworked condensed deposits because they are rich in glauconite and formed in response to deepening above a ravinement surface. The initiation of bedform development is likely to have occurred as the result of amplification of tidal currents due to the interaction of rising relative sea level and the geometry of the transgressed landscape. The area around Manitou Springs must have been a large embayment in the Cambrian shoreline that had a funneling effect on tidal currents and possibly also locally created geochemical conditions (i.e., slightly reducing) that favored glauconite formation. Myrow (1998) calculated a minimum water depth for the tidal dune deposits of 21 m based on preserved bedform height. The transgression was therefore of significant magnitude, given that there is only 3.1 m of section between the surface with desiccation cracks and the base of the dune deposits.

The nearly symmetrical geometry and low dips of stoss and lee sides of the middle Sawatch deposits resemble modern tidal dunes (e.g., Fenster et al., 1990) that form under nearly symmetrical tides. Deposits of such dunes (Allen's [1980] Class V and VI) are not well known from the ancient sedimentary record. The uniform NNW dips of the large-scale foresets may represent the orientation of the dominant tidal current (flood or ebb), as tidal dunes are generally flow-transverse. Large-scale bedform migration resulted from net accumulation over many tidal cycles. Because sediment transport increases exponentially with increasing shear stress (Middleton and Southard, 1984), small tidal asymmetry could have produced net transport with the dominant tide, and thus led to consistent large-scale, bedform migration directions.

The greater scatter in the paleocurrent data of small-scale cross bedding, formed by superimposed dunes (Fig. 3B), is similar to modern tidal dunes (Houbolt, 1982; Fenster et al., 1990; Davis et al., 1993). This is a reflection of the highly unsteady and nonuniform nature of the currents at the base of tidal flows. A large percentage of the smaller dunes migrated directly up and down the dune faces. This may indicate that the high threshold velocities required to move the coarse sediment of these dunes may have only been exceeded during peak flow conditions, during which time secondary flow may have been oriented nearly perpendicular to the dune crests.

Interpretations of depositional environments are difficult for the rest of the upper member because it lacks diagnostic sedimentary structures. The lack of wave- or storm-diagnostic features, and the abundance of trough cross stratification, indicate that tidal currents may have continued to influence deposition. Coarse quartz-rich sand was likely mixed with locally derived grains of carbonate and glauconite during episodic flooding events. The upper member shoals to the Cambrian–Ordovician mid-*Rossodus* unconformity, as indicated by an upward increase in abundance of trough cross-stratification and flat-pebble conglomerate and much less evidence of bioturbation.

Uplift and the Mid-Rossodus Unconformity

Myrow et al. (2003) significantly revised the stratigraphic assignment of the Cambrian units at Stop 1 (Fig. 4). Berg and Ross (1959) initially assigned glauconitic, mixed siliciclastic and carbonate deposits that rest above basal white quartz sandstone of the Sawatch Formation, and below carbonate of the Manitou Formation (Fig. 5), to the Peerless Formation, and subsequent authors followed suit (Noblett et al., 1987; Myrow et al., 2003). The glauconitic strata at Illinois Gulch near Woodland Park, Colorado, a short distance northwest of Stop 1, yielded an Upper Cambrian "Franconian" trilobite assemblage. North American strata of this age are now assigned to the lower Sunwaptan stage (Ludvigsen and Westrop, 1985; Westrop, 1986). The Peerless Formation, a unit exposed in the Mosquito and Sawatch ranges of Colorado, is a mixed siliciclastic and carbonate unit that also underlies the Ordovician Manitou Formation. There was little or no biostratigraphic control on this unit until Myrow et al. (2003) recovered conodonts from its type section on the flanks of Horseshoe Mountain next to the Peerless Mine. Their data established that at least the top 4 m of the 20.5-m-thick Peerless Formation contain conodonts of the *Eoconodontus* Zone (lower *E. notchpeakensis* Subzone) of the Upper Cambrian. These conodonts are considerably too young to be correlated with the lower Sunwaptan strata in the Front Range. The top of the Peerless Formation was shown to record an unconformity with Lower Ordovician Manitou Formation strata (*Rossodus manitouensis* Zone conodonts) above (Myrow et al., 2003).

Berg and Ross (1959) demonstrated, by faunal and stratigraphic patterns, that a major unconformity exists between their

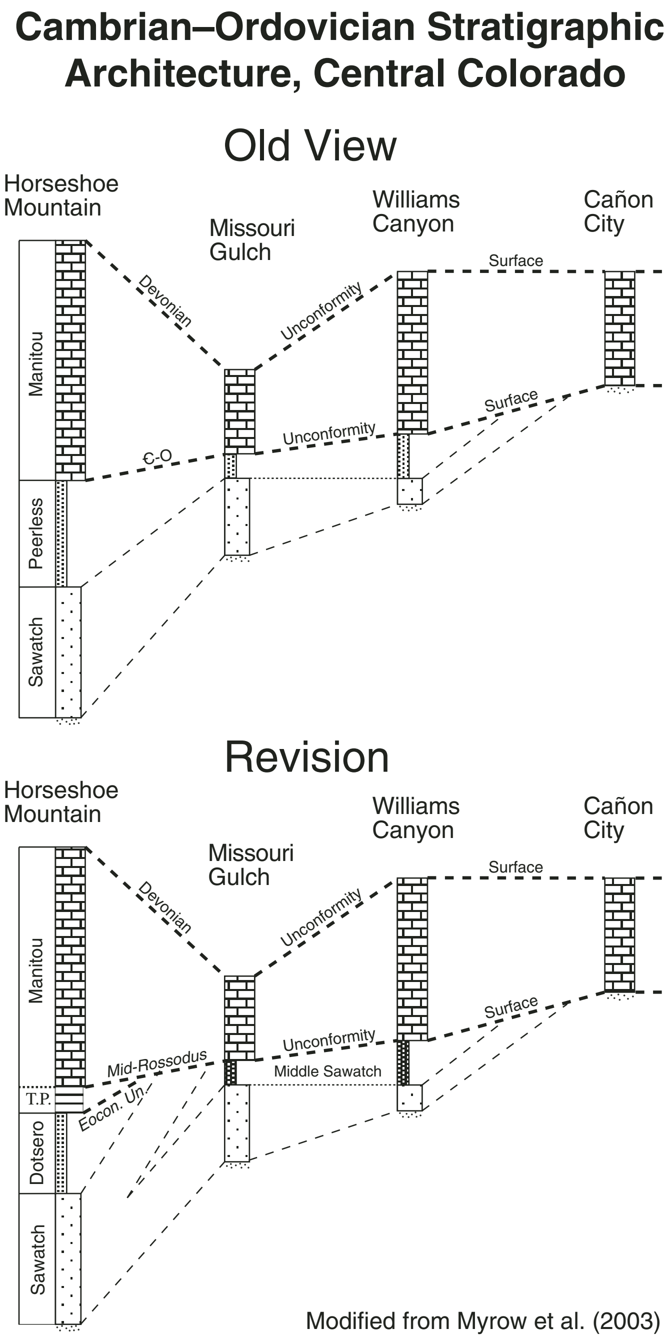

Figure 4. Cambro-Ordovician stratigraphic architecture, central Colorado: Comparison of correlation schemes for the Front Range and Mosquito Range. The "Old View" (Berg and Ross, 1959) correlates glauconitic and dolomitic deposits along the Front Range (Missouri Gulch, Williams Canyon, and Deadman's Canyon) with the Peerless Formation, whose type section is exposed at Horseshoe Mountain. Conodonts recovered from the Peerless at the type section indicate a much younger age, and hence the Front Range deposits are correlated with the glauconite-rich middle member of the Sawatch Formation, in the Revision (modified from Myrow et al., 2003).

"Peerless" Formation and the overlying Manitou Formation in the Front Range. They showed that uplift in southern Colorado prior to deposition of the Manitou Formation caused progressive erosional cut-out of the Cambrian units toward the south, and subsequent onlap and younging of the basal Manitou Formation from north to south (Fig. 4). In localities south of Colorado Springs, such as Cañon City, the Manitou Formation rests directly on Proterozoic granite, where the basal beds presumably contain the youngest onlapping strata of the formation.

Because the *Rossodus* age strata of the Manitou Formation rest unconformably on older *Eoconodontus* Zone rocks at Horseshoe Mountain to the northwest, Myrow et al. (2003) interpreted that unconformity to correlate with the Cambrian–Ordovician disconformity along the Front Range. Thus, both the "true" Peerless Formation and the upper quartzite member of the Sawatch Formation were removed along this "mid-*Rossodus* unconformity" in Front Range exposures (Myrow et al., 2003), including the exposures at Stop 1. The highly glauconitic unit that Berg and Ross (1959) identified as "Peerless" Formation in the Front Range is in fact the middle member of the Sawatch Formation (Fig. 4), a unit with similar lithologic characteristics to the Front Range "Peerless" Formation. Careful examination of the type section of the Peerless Formation, however, reveals that it contains little glauconite and is therefore not that similar lithologically to the Front Range deposits. Further, Myrow et al. (2003) reassigned the Peerless Formation strata to the Dotsero Formation, which is exposed across western and central Colorado. The middle member of the Sawatch Formation had never been

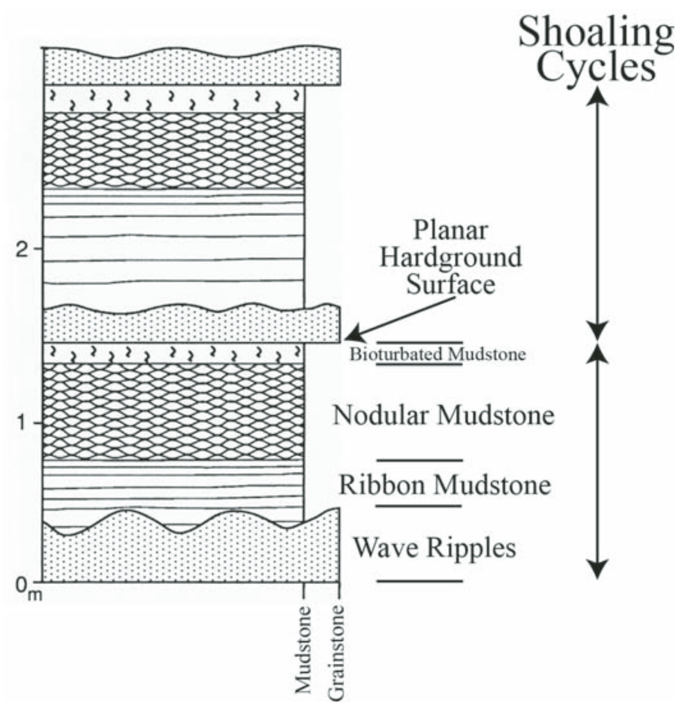

Figure 5. Generalized shoaling cycles in the lower Manitou Formation (optional Stop 1B).

identified in areas southeast of the Homestake shear zone of the Sawatch Range (see Allen, 1994), but only because it had been misidentified as the Peerless Formation along the Front Range. The middle member of the Sawatch Formation is not present in the central part of the state, in the Mosquito Range and parts of the eastern Sawatch Range, but occurs with increased glauconite content toward the west. The distribution of glauconite in the middle Sawatch Formation across the state would therefore indicate a general deepening both eastward and westward from the Sawatch and Mosquito Range area.

Carboniferous Strata—Paleoenvironments and Onset of Ancestral Rockies Orogeny

Mississipian Strata Exhibiting Paleokarst Features

Hardscrabble Limestone description. In Manitou Springs, the Mississippian Hardscrabble Limestone (Stop 2a) is age-equivalent to the famous Leadville Limestone. Medium-bedded carbonate mudstone is partially dolomitized (brown color) and devoid of macrofauna. Outcrops contain paleokarst collapse breccia consisting of subangular to angular clasts of carbonate mudstone of similar composition and texture to the host rock.

Hardscrabble Limestone interpretation. The strata record suspension deposition of fine-grained carbonate mud in a shallow marine setting. The lack of internal sedimentary structures or macrofauna precludes a more sophisticated paleoenvironmental analysis. The paleokarst breccia records exposure and the formation of karst caves by dissolution under meteoric water. This exposure marks a sharp stratigraphic transition to the overlying Glen Eyrie Shale Member of the Pennsylvanian Fountain Formation (Finlay, 1907).

Glen Eyrie description. The Glen Eyrie member of the lower Fountain Formation consists of organic-rich shale, siltstone, and quartz arenite (Suttner et al., 1984) (Stop 2b). The thin to medium quartz sandstone beds are well lithified and display circular plant trace fossils of *Lepidodendron* (Jennings, 1980), a common Carboniferous spore-bearing plant. There is spectacular preservation of an anchoring *Stigmaria* (root-like) structure, showing a characteristic diamond-shaped, bark-like surface and slender remarkably well preserved tapering projections. The projections may have acted more like leaves than roots, and given the shallow burial of the *Stigmaria*, they may have projected above the surface and been capable of photosynthesis. Indications are that the circular trace fossils were produced by penetration of growing projections, similar to those preserved on the *Stigmaria* fossil on the large slab. Fossil fragments of echinoderms, including crinoids and a sea-urchin-like creature, *Archaeocidaris dininnii*, together with conodonts and ostracods also have been found (Chronic and Williams, 1978).

Glen Eyrie interpretation. *Lepidodendron* is a fossil of an extinct plant that is related to the spore-bearing club mosses and ferns. Technically, they are most closely related to a group of plants of the order Isoetales, which are commonly known as quillworts. Spore-bearing plants reproduce in moist conditions, and the nature of the shale facies in this outcrop would support a waterlain organic-rich environment of deposition. The invertebrate fossil fragments indicate a marine or estuarine setting. The sandstone beds likely represent small fluvial channels that crossed the swampy and/or estuarine setting, transporting and depositing sand and large pieces of woody debris that would have washed into the depressions. The stratigraphic transitions from marine limestone (Hardscrabble Formation) to the swampy or estuarine setting of the Glen Eyrie Shale member to the thick alluvial fan deposits of the overlying part of the Fountain Formation record the onset of the Ancestral Rockies uplift. It is unclear whether the paleokarst of the Hardscrabble developed while the unit was exposed subaerially, or during initial deposition of the Glen Eyrie Shale. In any case, the Glen Eyrie is in a general sense a transitional succession sandwiched between marine and terrestrial lithofacies. Regression may have largely been a response to incipient uplift of the mountains along range-bounding faults at this time. New U-Pb isotope geochronology for detrital zircon from a quartz sandstone in the Glen Eyrie Formation (see below) supports this interpretation. Detrital zircons evidently do derive from a local source in the Central Front Range arc sequence, albeit with a notable absence of Pikes Peak Granite–aged zircon (ca. 1.08 Ga). The paucity of ca. 1.0 Ga zircon is surprising in light of the predominance of Pikes Peak Granite–derived coarse clastics in the Fountain Formation conglomerates (Suttner et al., 1984) (Stop 4). Potentially the Glen Eyrie–Fountain conglomerate units record unroofing in response to progressive displacement on the ancestral Ute Pass fault during formation of the Ancestral Rocky Mountains, with early exposure of Paleo- and Mesoproterozoic basement followed by eventual exhumation of latest Mesoproterozoic Pikes Peak Granite, and a significant disconformity at the top of the Glen Eyrie member.

Basement-Hosted Sandstones—Two-Part Classification, Depositional Setting, and Time of Emplacement

Tabular Sandstone Bodies

Within the Ute Pass fault zone in the Front Range (Fig. 1), tabular sandstones occupy fault-bounded panels (Scott and Wobus, 1973; Keller et al., 2005; cf Dokal, 2005) that form elongate ridges up to or exceeding 2 km in length, 500 m width, and 150 m in relief along the west margin of the Woodland Park graben (Temple et al., 2007). The large sandstone bodies are spatially associated with sandstone dikes hosted by granite or gneiss, but contacts between the sandstone bodies and dikes are only rarely found. Temple et al. (2007) describe a strike ridge of the competent sandstone that forms a prominent feature in the landscape of Woodland Park, Colorado, and they depict another as an element within a duplex structure on the geological map. In Chrystola, Colorado, a sandstone body forms a hogback bordered by granite on both sides; this occurrence is featured in a GSA field guide by Ross et al. (2010). At these locations, subvertical bedding or pseudobedding is evident. A third locality, featured on this field trip, is north of Sutherland Creek in Manitou Springs (Stop 3; Fig. 1). The sandstone at this location exhibits weak to moderately well-developed subhorizontal partings (Fig. 6A), and it is intruded by dikes and sills that pass upward across a low-angle fault into Proterozoic crystalline rocks. Occurrences of basement-hosted dikes elsewhere in the Front Range (Scott, 1963; Dockal, 2005) are not spatially associated with the Ute Pass fault.

Previous investigators of the Front Range dikes (Cross, 1894; Crosby, 1897; Harms, 1965; Hoesch, 2008; Dulin and Elmore, 2013) have considered the fault-bounded sandstone bodies, dikes, and sills to all be intrusive. A description of outcrop features and aerial extent of the sandstones, together with the questions of sediment source and emplacement mechanism for sandstone intrusions, were introduced in the works of the 1890s. Crosby (1897) observed the homogeneous nature and an absence of stratification in the sandstones. This characteristic presents a distinction from Sawatch Formation, as was later noted also by Temple et al. (2007). Harms (1965) examined the dikes from the standpoints of sedimentology and of paleostress environment for development of tensile structures with bearing on Front Range fault geometry and dynamics of Laramide uplifts. He concluded that Sawatch sandstone was the principal sediment source, and, based on geometrical and dynamic analysis, Harms concluded that sandstone dike emplacement probably occurred during the Laramide orogeny. The work of Harms (1965), augmented by outcrop observations of primary dike fabrics with bearing on permeability and porosity, is revisited by Hoesch (2008), who made a case for the petroleum resource potential of the Ute Pass fault clastic dikes.

Recognizing that early workers did not have the advantage of the contemporary understanding of mass transport deposits (Shipp et al., 2011), sand injectites (e.g., Hurst et al., 2011), and plate tectonic theory that has been achieved through technological advances in geophysics, this field guide directs those readers who have interest in the initial hypotheses to the original works.

Kost (1984), Dulin and Elmore (2013), and Freedman et al. (2012) employed paleomagnetism in efforts to derive the timing of dike emplacement, insofar as the primary rock magnetization could indicate a paleomagnetic pole position within the well-constrained North America apparent polar wander path (e.g., Weil et al., 2004). A conventional determination of the absolute age for the sandstone intrusions presents obvious difficulties because the dikes consist of detrital material derived by erosion of an older source rock and they lack cogenetic radiogenic mineral phases of the sort that are used for radiometric dating of igneous intrusions. The dikes record a complex magnetization history, with multiple magnetization vectors acquired in the late Paleozoic or before, including a possible Neoproterozoic to early Cambrian component (Kost, 1984; Dulin and Elmore, 2013). They establish with reasonable certainty that the sandstones are pre-late Paleozoic, albeit with an unresolved issues of structural correction due to Ute Pass fault footwall rotations of uncertain magnitude and orientation, and of the possibility that a widespread late Paleozoic remagnetization (Geissman and Harlan, 2002) obscured the primary magnetization record of the dikes.

The tabular sandstones distributed along the Ute Pass fault (Fig. 1, Stop 3) (Scott and Wobus, 1973; Keller et al., 2005; Temple et al., 2007) have many descriptive characteristics in common with sandstone dikes (Stop 5), together with important distinctions that lead to our formulation of an integrated model for a genetic relationship. Description and interpretations of the tabular sandstone bodies and sandstone dikes, presented here, are based on field study over a broad area.

Sandstone bodies—description. The sandstone is massive and for the most part structureless, with isolated rounded quartz granules and pebbles (0.5–5 mm) supported within a

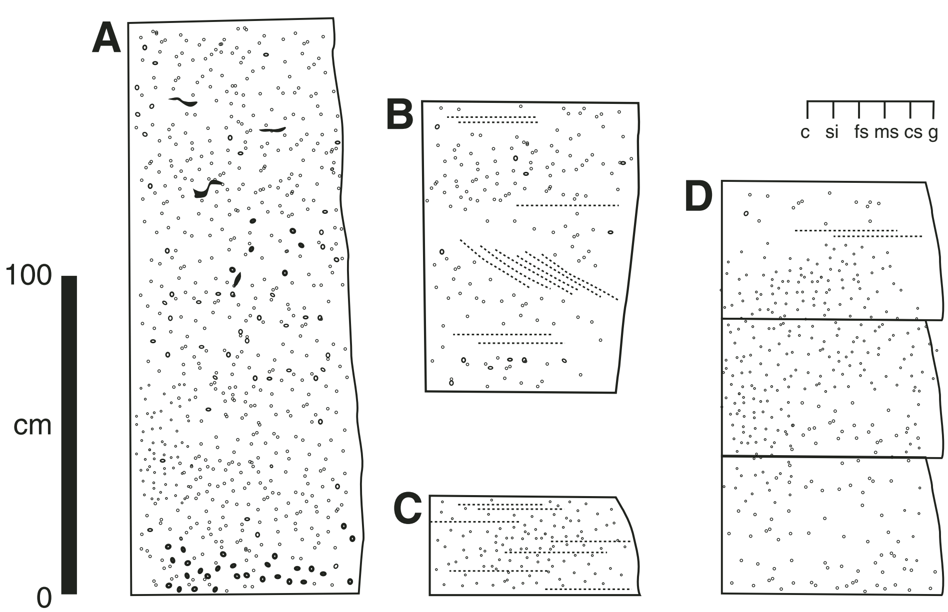

Figure 6. Representative lithofacies of the tabular sandstone bodies along the Ute Pass fault: (A) structureless granule- and pebble-bearing massive sandstone; may exhibit diffuse grading in respect to matrix grain size and dispersed class size (over a thickness of meters). (B) Massive, granule-bearing, medium- or fine-grained sandstone with indistinct, unbounded cross beds and sparse discontinuous subhorizontal parallel laminae. (C) Structureless fine sandstone with dispersed matrix-supported granules to pebbles, systematic but discontinuous partings spaced ~0.5 m to 3 m that are suggestive of meter- or meters-scale bedding, albeit with no evident differences in structure of the sandstone on either side of the partings. (D) Structureless fine sandstone with dispersed, matrix-supported granules to pebbles, exhibiting planar partings attributable to bedding or pseudobedding.

Figure 7. Field photographs illustrating (A) dispersed, matrix-supported pebbles within a Tava sandstone body and (B) coarse sandstone with dispersed quartz granules within an intrusive dike.

matrix of medium, fine, or very fine sandstone (Figs. 6 and 7). Very sparse, small, tabular flakes of claystone or mudstone may be found among the "floating" clasts. The sandstone consists dominantly of quartz, with accessory (<3%) K-feldspar, plagioclase, micas, and magnetite. Detrital zircon is abundant. The degree of induration varies. Rounded quartz cobbles up to 7 cm are rarely observed. In one instance, a group of eight non-touching cobbles (>4 cm length) was observed in the center of a dike.

In places, planar partings suggestive of meter- or meters-scale bedding are observed within the massive sandstone bodies (Fig. 8); however, grading and sorting are very weak to absent, and no evident distinction exists between the sandstone on either side of the planar breaks. If sorting by size of the dispersed grains and pebbles, or the matrix sand, exists, it must be over a thickness of meters to decimeters, a possibility that is being explored with ongoing research. The planar structures (pseudobedding) are recorded as bedding attitudes on two

Figure 8. Systematic subvertical partings deemed to be "pseudo-bedding" in the fault-bounded sandstone body along the Ute Pass fault at Chrystola (see Stone, 1880s, www2.coloradocollege.edu/library/specialcollections/manuscript/stone/129.html; accessed June 2013). In this outcrop, there are oblique slickenlines upon the steeply dipping planes, an indication that the observed planes do not correspond to primary bedding.

quadrangle maps (Keller et al., 2005; Temple et al., 2007); however, field examination reveals the presence of brittle slip lineations (slickensides) upon many of the surfaces (e.g., Chrystola and Manitou Springs), so the origin of the partings as primary sedimentary structures is in question.

Secondary characteristics of the sandstones are: (1) Varying degree of cementation, with hematite cement most common and calcite cement found rarely. Quartz cement is lacking, but quartz grain impingement and suturing is observed rarely in thin section. (2) A wide range of sandstone color, including purple-red, pale purple, white, yellowish white, rusty, brown, or red. Red and/or white patchy coloration and mottling is common. Weathered surfaces may be gray, orange, or purple-red (due to oxidation/reduction of hematite). (3) A brittle deformation overprint is evident at most localities, in the form of slickenside surfaces and faults of small displacement (<0.5 m) (Fay and Siddoway, 2004); however, areas of sandstone with minimal brittle deformation also may be found.

Sandstone bodies—interpretation. It is difficult to interpret the depositional mechanism for structureless sandstones in the rock record in detail because of the absence of visual features that provide information about flow (Duller et al., 2010). However, the sedimentology of massive structureless sandstones is most consistent with sediment-gravity deposition of large-volume sand slurries in hyperconcentrated flows capable of entraining and supporting granule and pebble clasts (e.g., Gruszka and Zieliński, 1966; Mulder and Alexander, 2001; Duller et al., 2010). The scale and distribution of the large sandstone bodies suggest that they originated in a depocenter with considerable accommodation space, likely a narrow fault-controlled trough. We speculate that the units resulted from aggradation of sand beneath channelized turbulent flows within a narrow structural basin along the ancestral Ute Pass fault. Hyperconcentrated flows are indicative of rapid sedimentation in a tectonically active environment affected by high precipitation that may be prone to liquefaction and gravitational destabilization (e.g., Jolly and Lonergan, 2002) in response to seismic activity or through sedimentary loading (e.g., along the ancestral Ute Pass fault). The absence of other facies associated with the depositional mechanism may be attributed to (1) Ute Pass fault deformation and preferential preservation of competent sandstones, or to (2) enhanced chemical weathering that was a consequence of distinctive Proterozoic ocean and atmosphere chemistry (e.g., Jones et al.,)

The presence of sandstone sills and dikes in proximity to, or cutting, the sandstone bodies suggests that volumes of sand periodically were destabilized, leading to fluid escape of formation water and sand from high-porosity sand deposits with metastable grain distribution (e.g., Hurst et al., 2011). Disruption arising from pore fluid escape (liquefaction) may account for some of the lack of internal structure in the tabular sandstone bodies. It is unlikely that the large sand bodies themselves formed as sedimentary dikes because of the enormous volume of sand and water required to emplace a single intrusive body of such dimensions (>24 million m^3 of water and >50 m^3 of sand based on Hurst et al., 2011, parameters), much less the full Ute Pass fault sandstone array. With further research, if it can be shown that the tabular sandstone bodies are intrusive, then the possibility of shear-induced liquefaction triggered by a bolide impact (e.g., Cartwright, 2010) will need to be explored.

Clastic Dikes

Dike description. Near-vertical dikes and sills are hosted by Pikes Peak Granite, foliated Routt Plutonic units (see Tweto, 1987), and older gneiss. Widths range from one centimeter to over four meters in width. Individual dikes have a lateral extent of exposure of 2–15 m, before they disappear beneath cover or are truncated by younger faults. However, one array of 3–5 dikes has been mapped over a lateral distance of 6 km across North and South Cheyenne Cañon and the east flank of Cheyenne Mountain (Fig. 1; stop 5). Multiple generations of dikes are evident on the basis of sharp crosscutting relationships at three known localities, and sandstone bodies are cut by dikes at three known localities (see Stop 3). Dikes and sills crosscut diabase dikes hosted by Proterozoic gneiss at Cheyenne Cañon and Cheyenne Mountain.

The majority of intrusions have planar margins, with subvertical geometry. Sills of thickness 1 m or less also are observed. The sedimentary intrusions consist of fine-, medium- or coarse-grained, rounded to subrounded quartz sand, with accessory minerals <3%, based on petrographic examination of hand specimens and thin sections. Dikes along the NW-trending portion of the Ute Pass fault zone contain dispersed granules, pebbles, and rare cobbles throughout. Elongate, angular clasts (xenoliths) of the crystalline host may be present, with the long dimension of such clasts (up to 20 cm in length) parallel to dike margins in most instances. Often the shape of a large crystalline clast displays a geometrical "fit" to the shape of the dike margin.

Sandstone dike interpretation. The massive, largely structureless fine- to medium-grained sandstone that contains isolated quartz granules, pebbles, and cobbles is best understood as a sand injectite emplaced as over-pressured fluidized sand (Hurst et al., 2011) into planar fractures in the crystalline host rock. This interpretation is corroborated by anisotropy of magnetic susceptibility results that yield prolate to oblate ellipsoids parallel to dike margins, with, in one instance, strongly prolate subhorizontal fabrics associated with margin imbrication (Freedman et al., 2012; Freedman, 2013).

Conditions for injection of fluidized sand developed at least two times, based upon the occurrence of crosscutting dikes and/or sills. We interpret that elevated pressures developed due to metastable packing of sandy sediments emplaced as hyperconcentrated flows (e.g., Hurst et al., 2011) deposited in a narrow structural basin along an active ancestral Ute Pass fault, with vigorous erosion and sediment transport from an upthrown block. Gravitational loading due to rapid sedimentation or seismicity may have destabilized the sands and triggered dike emplacement. The water-rich environment that provided the necessary volume of formation water may have arisen in a marine setting (Jolly and Lonergan, 2002), a continental setting subject to high precipitation (Hurst and Glennie, 2008), or in a realm of warm-based continental glaciation (e.g., Le Heron and Etienne, 2005) to glaciomarine deposition (e.g., van Loon, 2008).

Due to the close similarities in sedimentological characteristics, and the close spatial association and crosscutting relationships between the sandstone bodies and dikes, an integrated model is envisioned wherein the large massive sandstone bodies, formed as sediment gravity deposits, represent parent bodies that were occasionally destabilized, leading to catastrophic emplacement of over-pressured fluidized sand injectites into preexisting large fractures within the basement. The systematic fractures in Pikes Peak Granite, into which sandstones were injected, may have originated prior to the injection event (e.g., Morgan et al., 2002).

The descriptive characteristics of the massive sandstones and dikes markedly differ from those of Sawatch Formation (see above), a concern that has been raised by Temple et al. (2007) and J. Temple (2008, personal commun.) on the basis of field criteria. The sedimentary features suggest a mode of deposition utterly unlike that of the Sawatch Formation. As a consequence of these distinctions, we propose the name "Tava sandstone" for the massive near-structureless sandstones within fault-bounded panels and intrusive dikes along the Ute Pass fault. *Tava* is the original name for Pikes Peak in the language of the indigenous Tabeguache Ute (Pikes Peak Historical Society, www.pikespeakhsmuseum.org/PPHS/Main%20Headings/Ute%20Indians.htm, accessed June 2013), thus the proposed formation name references the spatial distribution of the sandstones around the perimeter of the Pikes Peak massif.

Time and Tectonic Context for Emplacement of Tava Sandstone Dikes

The determination of the absolute age for the sandstone intrusions presents difficulties because the dikes consist of detrital material derived by erosion of an older source rock (and they lack cogenetic radiogenic mineral phases of the sort that can be used for radiometric dating of igneous intrusions). Attempts to derive a younger age limit by determination of a paleomagnetic pole position (Kost, 1984; Dulin and Elmore, 2012; Freedman, 2013) are hindered by a need for structural corrections (Freedman, 2013) due to shearing and rotation in the Ute Pass fault zone, and by the pronounced but potentially variable effects of regional remagnetization in Pennsylvanian time (Geissman and Harlan, 2002).

A new possibility for resolution of the question of dike emplacement age is the detrital zircon provenance for the Tava sandstone bodies and dikes (Siddoway et al., 2013; Fig. 9). Three samples of Tava sandstone and one comparison sample of quartz arenite from the Glen Eyrie Shale were analyzed, to obtain relative age-probability curves that may be compared to the western USA reference curves for Mesoproterozoic to Cambrian arenites (Stewart et al., 2001) augmented by new detrital zircon data for Cambrian units in New Mexico (Amato and Mack, 2012). The western USA reference curves reveal that quartz arenites derived from local sources are distinguished by *narrow, sharp peaks* in the age spectra, whereas a broad spread of zircon ages between 1.2 and 1.0 Ga is diagnostic of arenites of distant derivation from the Grenville orogen (Stewart et al., 2001; e.g., Amato and Mack, 2012). In Colorado, local basement sources such as the Colorado Front Range arc sequence (ca. 1.72 Ga; Fisher and Fisher, 2004)

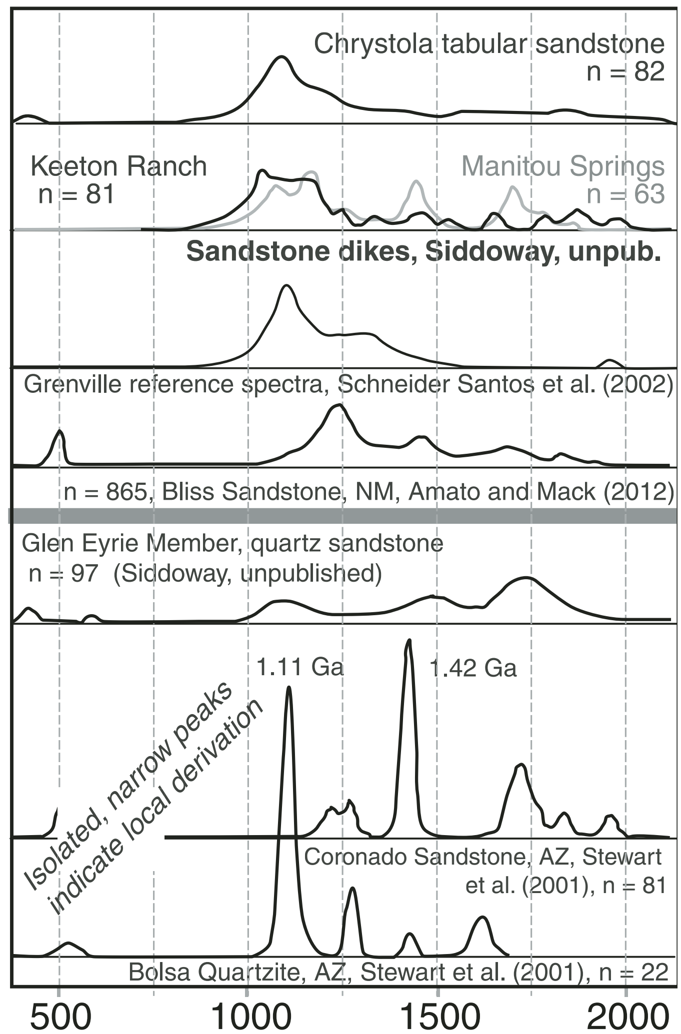

Figure 9. Comparison of detrital zircon relative age-probability curves for Tava sandstone with reference curves (Stewart et al., 2001; Amato and Mack, 2012). The broad spread of 1.2–1.0 Ga zircon ages is characteristic of Mesoproterozoic to Cambrian arenites of the western United States (Stewart et al., 2001). Contrasting spectra come from quartz sandstone of the Pennsylvanian Glen Eyrie Member, which exhibits isolated, narrow age peaks at ca. 1.48 and 1.72 Ga, with an absence of evidence of ca. 1.08 Ga zircon derived from Pikes Peak Granite. The pronounced distinction in detrital zircon provenance provides support for the interpretation that the Tava sandstone is not Pennsylvanian, and thus is unrelated to the Ancestral Rocky Mountains orogeny.

and Pikes Peak Granite (ca. 1.08 Ga) would produce an abundance of zircon to be reflected in sharp, narrow peaks (Stewart et al., 2001, see Fig. 9, lower).

One large tabular body from Chrystola, Colorado, and two sandstone dikes of Tava sandstone (Siddoway et al., 2013) yield significant populations of detrital zircon between 1.10 and 0.97 Ga that potentially were derived from Pikes Peak Granite or its hypabyssal to extrusive equivalent, the Keeton Porphyry (Murray, 1975; Sanders, 1999), or from distant sources in the Grenville orogen (Stewart et al., 2001). Equally or more abundant, however, are zircons of 1.15–1.2 Ga age that have no source in the Rocky Mountain region. Together, the populations form a mixed population that appears as a broad spectrum within which there is a narrow peak, on age-probability curves (Fig. 9). The pattern resembles that obtained for Neoproterozoic–Cambrian sandstones of the Rocky Mountains that derived from erosion and transport of sediments from the Grenville orogen (Stewart et al., 2001; Amato and Mack, 2012). The age patterns for Tava sandstone samples differ sharply from those of a quartz sandstone from the Glen Eyrie member of the Pennsylvanian Fountain Formation, which display sharp isolated peaks of ca. 1.72 and 1.48 Ga, and a notable absence of zircon of ca. 1.08 Ga Pikes Peak Granite age (Fig. 9).

The distinctions among the detrital zircon spectra (Fig 9) for Tava sandstone samples from Chrystola, Manitou Springs, and Keeton Ranch samples (Fig. 1) are also of potential significance. For example, the pronounced younger peak for the Keeton Ranch sample may reflect a local source in Keeton Porphyry (Sanders, 1999) at the site. The pronounced peak at ca. 1.45 Ga for the Manitou Springs sample may reflect derivation from a nearby source in Berthoud Suite plutonic rocks (Tweto, 1987) in Colorado.

In summary, the detrital zircon provenance data strongly suggest that the Tava sandstone is Cambrian or Neoproterozoic in age. Although the Ute Pass fault zone–associated sandstones are, already, classified as Cambrian strata on most geologic maps (e.g., Scott and Wobus, 1973; Morgan et al., 2002; Temple et al., 2007), the pronounced differences in sedimentology and paleoenvironment of deposition between the Sawatch Formation (Stop 1) and Tava sandstone (Stops 3 and 5), call into question the direct correlation of the two (e.g., Harms, 1965; Scott and Wobus, 1973; Hoesch, 2008). In an effort to resolve this issue, a study of detrital zircon provenance for Sawatch Sandstone is under way, and it may offer the means to determine whether a correlation between the two units is valid. For the time being, field trip participants will have an opportunity to reach their own conclusions based on the observational criteria they acquire at Stops 1, 3, and 6.

If sandstone deposition and dike emplacement occurred during a period of tectonism that caused the formation of a regional fracture array, the topographic gradient for sediment transport, and/or the existence of the inferred fault-controlled basin, the following candidates for tectonism may be contemplated (Siddoway et al., 2009): (1) Neoproterozoic rifting of Laurentia, (2) Cambrian Oklahoma Aulacogen, with extent into Colorado, (3) Pennsylvanian Ancestral Rocky Mountains orogeny, or (4) Cretaceous–Tertiary Laramide orogeny. An *older* age limit is of course provided by the time of intrusion of the Pikes Peak Granite (1.08 Ga) that hosts Tava sandstone.

The latter two events can now be ruled out. The sparsity of Pikes Peak Granite arkosic detritus in the Tava sandstone compared to Laramide synorogenic sediments (D1 and D2 of Raynolds, 2002), the absence of Pikes Peak Granite–aged detrital zircon in the Chrystola sample, and the broad spectrum of Mesoproterozoic detrital zircon in all three Tava samples prove that the Tava sandstone cannot be associated with the Laramide, as has been suggested by Harms (1965). Further support comes from the delimitation, through current paleomagnetism research, of primary and secondary magnetizations that are Pennsylvanian or older (Dulin and Elmore, 2013; Freedman et al., 2012). A temporal and genetic relationship of the Tava sandstone with the late Pennsylvanian Ancestral Rocky Mountains orogeny (Freedman, 2013) can be ruled out, however, on the basis of the sharp difference in detrital zircon age spectra between Tava sandstone and Pennsylvanian Glen Eyrie sandstone (Fig. 9).

Existing detrital zircon data do not provide grounds to exclude either the Neoproterozoic or the Cambrian from consideration for the time of Tava sandstone emplacement. From the standpoint of tectonism that could induce tensile fractures and gravity-induced sedimentation that could lead to sandstone injection: (1) the formation of NW- to N-trending ancestral faults in the Rocky Mountain West has been attributed to Laurentia breakup in Neoproterozoic time (Timmons et al., 2001), and mass flow deposits are known from Neoproterozoic glaciomarine systems (van Loon, 2008). (2) Possible indications of Oklahoma aulocogen propagation into Colorado are Cambrian alkalic magmatism in Colorado (McMillan and McLemore, 2004; Schoene and Bowring, 2006; Pardo et al., 2008) and Cambro-Ordovician differential motion and/or erosion across faults in the Central Front Range (Houck et al., 2012; Kirkham et al., 2012).

Structural Geology of the Southern Front Range

Time of Formation of the Front Range Monocline

A structure that is attributed to the Laramide orogeny is the regional-scale Central Front Range monocline in Colorado Springs (Fig. 10) (Finlay, 1916; Erslev et al., 2004), that borders the Mesozoic basement-involved Front Range uplift developed in the Rocky Mountain foreland (Hamilton and Myers, 1966) from 80 Ma to 40 Ma (e.g., Bird, 1988). The specific fault and fold timing presents a conundrum that has been largely overlooked due to the casual attribution of such a broad time span for the Laramide orogeny. An impetus to explore the Front Range deformation timing more closely is provided by the discovery of a hiatus in deposition of Laramide synorogenic strata between 64 and 63 Ma and 54 Ma (Obradovich, 2002), suggesting the possibility that pulses of tectonic motion upon faults led to discrete events of enhanced erosion and deposition of coarse clastic material, or vice versa.

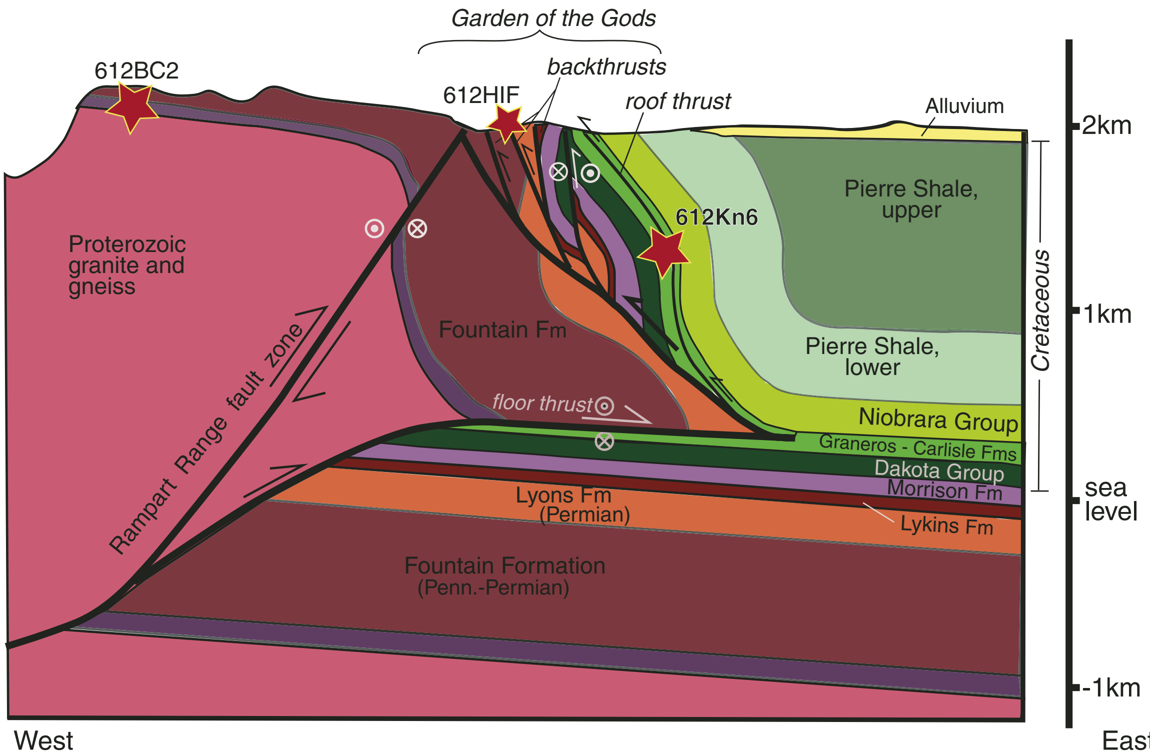

Figure 10. Structural cross section of the hinge zone of the Front Range monocline at Garden of the Gods, according to evolved triangle zone interpretation of Sterne (2006). Position for three of four illite age analysis (IAA) samples is indicated schematically by star symbols. Star symbol corresponding to sample 612HIF shows the location of the Hidden Inn fault (HIF). The profile shows the Rampart Range fault as a west-dipping, east-directed reverse fault that soles into a concealed floor fault at depth. The east-dipping subsidiary faults are shown to be west-vergent backthrusts that attenuate section. A roof thrust is interpreted within Pierre shale, with a fault attitude semi-parallel with bedding in the shale. The roof thrust is an element of a triangle zone model that offers a way to understand the seemingly contradictory east- and west-vergent reverse structures within a single structural system (e.g., Jones, 1996, Mackay et al., 1996; Sterne et al., 2006).

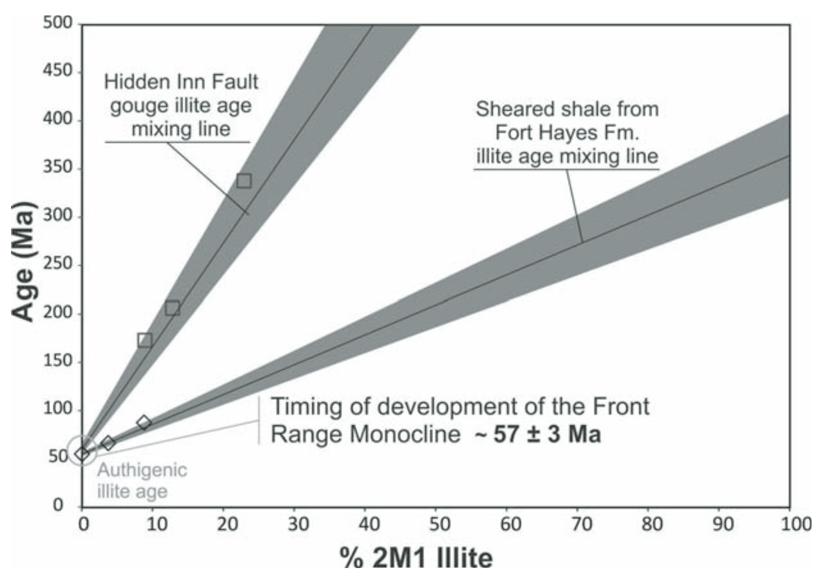

Figure 11. (A) Photo of clay gouge upon plane of Hidden Inn fault (Fig. 12). (B) York regression line for determination of the time of growth of shear-generated authigenic illite within two sites of structural significance for development of the Front Range monocline.

$^{40}Ar/^{39}Ar$ illite age analysis. To address the question of the specific timing of fault slip and ultimately of monocline formation, we undertook $^{40}Ar/^{39}Ar$ illite age analysis (IAA) of meticulously prepared, minute amounts of illitic clays extracted from fault gouge (e.g., van der Pluijm et al., 2001, 2006; Haines and van der Pluijm, 2008, adapted from vacuum-encapsulated Ar-Ar dating techniques of Foland et al., 1992). This approach accepts that fault gouge contains a mixture of detrital illite (minute flakes of muscovite or the 2M1 illite polytype) together with authigenic illite (1Md illite polytype) that grows in the fault zones as a consequence of enhanced fluid circulation and fluid-rock interaction triggered by fault slip and/or shear. For IAA, at least three grain size fractions containing different proportions of 1Md and 2M1 illite are analyzed (Fig. 11). The IAA method that we applied involves obtaining an illite polytype quantification and Ar-Ar age in each grain-size fraction analyzed. By plotting age versus percent 2M1 detrital illite for each grain-size fraction analyzed in a sample, it is possible to estimate the age of the authigenic illite formed during deformation by using York regression analysis, using the lower intercept of the age mixing line (modified by Mahon, 1996; see Haines and van der Pluijm, 2008 for details on the application of the method) (Fig. 11B). We applied IAA to samples as follows. Sample locations are shown in Figures 1 and 10.

- Fault gouge from the Hidden Inn fault (sample 612HIF), a west-vergent, steeply inclined reverse fault in the footwall of the Rampart Range fault;
- Thin shale layers interbedded with competent limestone or sandstone, affected by bedding-parallel shear during limb rotation within the steeply inclined limb of the Front Range monocline (sample 612Kn6 from Fort Hayes Limestone in Colorado Springs and sample 612Kd2 from Dakota Formation sandstone at the southern terminus of the Ute Pass fault footwall). Shear is evidenced by strong cleavage and lustrous surfaces termed nanocoatings (Schleicher et al., 2010).
- Strongly sheared, well-foliated, meter-wide, clay-rich horizon between limestone and orthoquartzite (Williams Canyon member of the Hardscrabble Limestone; Hill, 1983) within the gently dipping upper limb of the monocline (sample 612BC2) (Karlsson et al., 2013). Polytype characterization showed that sample 612BC2 consists dominantly of shear-related authigenic illite in the fine grain size fractions (<0.2μm), with a presence of detrital (2M1) illite in the coarser clay-size fractions (Karlsson et al., 2013).

Carbonate-shale successions were favored for sampling because the primary rocks have a low abundance of detrital illite, K-feldspar, or other K-bearing phases that may be difficult to separate from authigenic illite, and could affect the age determination (Fitz-Díaz and van der Pluijm, 2013). The samples of gouge (e.g., 612HIF) from the Hidden Inn fault that is bounded by microcline-rich conglomeratic rocks of the Fountain Formation (Fig. 11A) presented greater difficulties for sample preparation, but nevertheless painstaking clay separation methods yielded samples that contain 20% detrital illite or less (for all samples).

York regression analysis for the three analyzed samples from the steeply inclined limb of the Front Range Monocline in the Colorado Springs area (Figs. 1 and 10) yields the following authigenic illite age estimates: (1) 57.5 ± 5 Ma for the Hidden Inn fault that separates Lyons and Fountain Formations in Garden of the Gods (sample 612HIF); (2) 55.7 ± 1.6 Ma for subvertical sheared shale interbeds within the Fort Hayes limestone member of the Niobrara Formation (sample 612Kn6); and (3) 67.3 ± 2.6 Ma for authigenic illite in the sample collected from the Dakota Group. Preliminary results from the single sample from the upper, shallow limb of the monocline at Snyder Quarry (sample 613BC2, Fig. 11), provided (4) an authigenic illite age estimate >120 Ma.

Geochronology—Interpretation. This outcome of nearly identical age, within the error, for samples 512HIF and 612Kn6 (Fig. 11) indicates that bedding-oblique reverse faulting and bedding-parallel shear both occurred at the same time during deformation of strata within the steeply dipping limb of the Front Range monocline. The two results define a lower intercept of 57 ± 3 Ma, very close to the time of the younger pulse of Laramide synorogenic sedimentation at 54 Ma (Obradovich, 2002). The outcome contrasts with the chronostratigraphic results of Raynolds (2002), who attributes the older D1 and younger D2 synorogenic units of the Denver Basin (e.g., Dawson Conglomerate) to episodes of erosion due to reverse displacement and denudation along, respectively, the Rampart Range fault in Cretaceous–Tertiary time and the Ute Pass fault at the Paleocene–Eocene boundary. This discrepancy must be addressed through further IAA research with broader regional sampling of Front Range faults. The possibility that the Laramide fault activity has a temporal and genetic correlation to the Paleocene–Eocene Thermal Maximum (PETM) climate transition also demands investigation. The PETM at 55 Ma was marked by changes in precipitation, weathering, and sediment mobilization, causing gravitational unloading of range blocks that may have triggered bedrock uplift and structural activation and/or reactivation of Laramide faults (Fricke et al., 2012).

The result for southern sample 612Kd2 falls within the broad time span of the Laramide orogeny but is significantly older than the results from the Colorado Springs area, which might imply that deformation on the southern Ute Pass fault zone occurred earlier than deformation on the Rampart Range fault. The 612Kd2 illite age seemingly corresponds to the earlier, ca. 64 Ma period of Laramide synorogenic sedimentation identified by Obradovich (2002) for the Denver Basin; however, the evidence of Ute Pass fault activity at the Cretaceous–Tertiary boundary appears to contradict Raynolds' (2002) Denver Basin chronostratigraphy.

The IAA results from the gently dipping limb of the Front Range monocline at Snyder Quarry (sample 613BC2) offer insight not only into the timing but also the strain history in the area. The >120 Ma result raises the possibility of pre-Laramide deformation, previously undetected in the area. The preservation

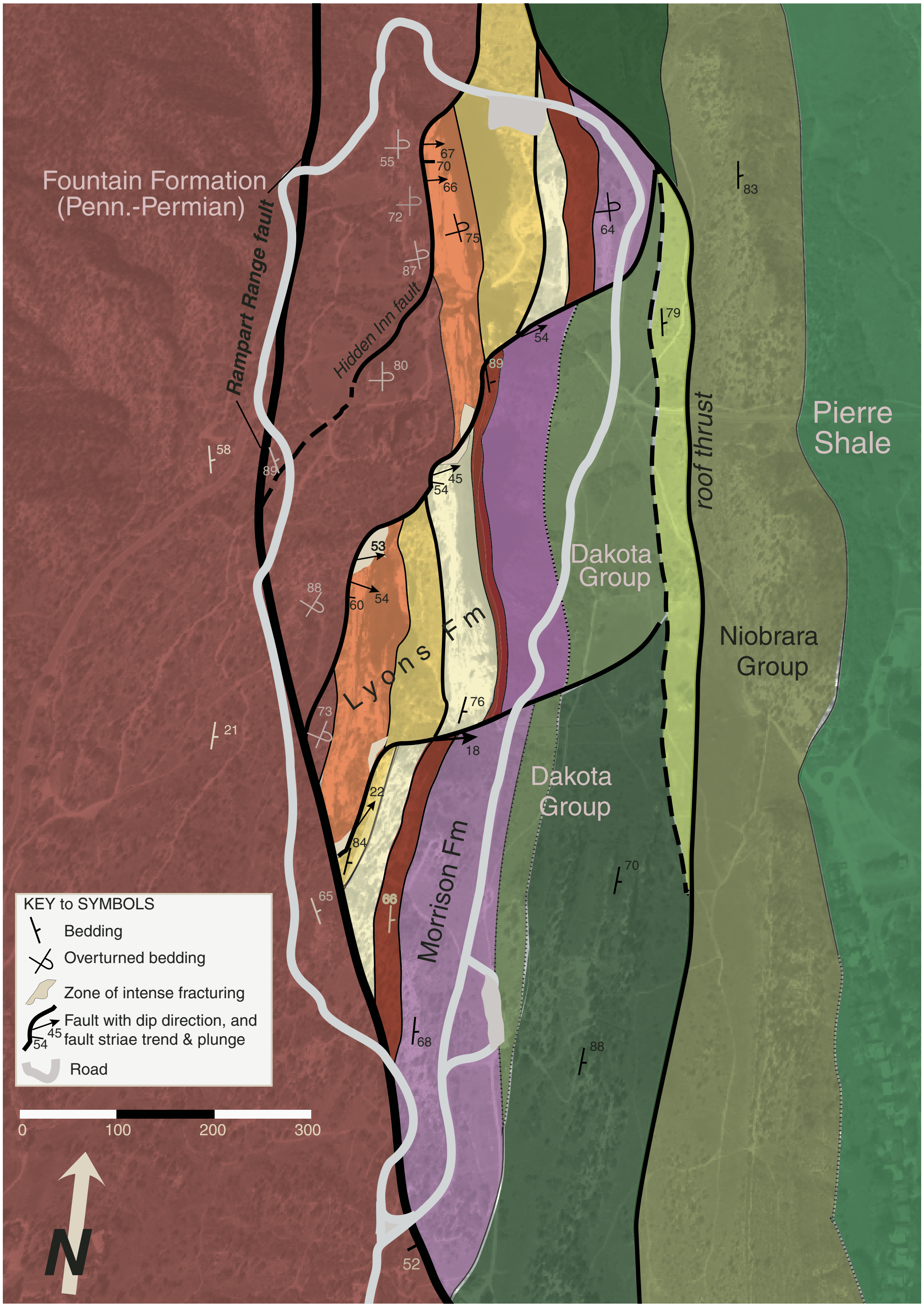

Figure 12. Geologic map of Garden of the Gods Park in Colorado Springs. Segmented faults within the footwall of the Rampart Range fault trend north to northeast. These and subsidiary brittle structures are the focus of this field trip. Participants will also have ample time to contemplate the triangle zone interpretation of Sterne (2006) for the southern Rampart Range fault zone (Fig. 10). Color designations for lithological units are as shown in Figure 10, with the exception of the Permian Lyons Formation that is subdivided into lower, middle, and upper members on the geologic map as a means to better provide structural markers for fault displacement.

of Jurassic–Cretaceous authigenic illite indicates that the upper limb of the Front Range monocline was inactive during Laramide deformation, and that Laramide strain was localized in the region of maximum bedding rotation on the steep limb and in the hinge zone of the range-scale fold. Additional IAA is being conducted to reduce uncertainty in the 613BC2 age in order to ascertain its significance. Complete results for authigenic illite from this sample and the interpretation of the age will be discussed during the field trip.

A more complete description and a discussion of the implications of the IAA ages for the evolution of the Front Range and the contemporaneity of the Front Range monocline with the synorogenic sedimentation in intermontane basins and with the Paleocene–Eocene Thermal Maximum will be presented during the field trip.

Structural Geology of Garden of the Gods Park

The Garden of the Gods (Fig. 12) (Stops 6 and 7) refers to an area of monoliths formed upon competent sandstones within the Pennsylvanian to Cretaceous sedimentary succession. The Fountain Formation coarse arkosic sandstone and conglomerate, lower and upper Lyons Formation quartz arenite, Dakota Group quartzose sandstones, and the Fort Hayes member of the Niobrara Group form the prominent ridges (Noblett, 2011). Bedding strikes ~north-south in Garden of the Gods, approximately parallel to the trace of the west-dipping Rampart Range fault that passes immediately to the west of the monoliths, through the hinge zone of the Front Range monocline. Bedding dips subvertically within the monocline's steep limb (Figs. 9 and 12). Just one kilometer to the east and west of Garden of the Gods, bedding dips are gentle to subhorizontal.

In the Rampart Range fault footwall in Garden of the Gods, close-spaced, steeply east-dipping reverse faults within subvertical bedding have up-to-the-west displacement that creates younger-upon-older age relationships (Fig. 10) (Sterne, 2006) that are counter to the customary age juxtaposition produced by reverse faults. Because the motion sense of the reverse faults is opposite to that of the Rampart Range fault master fault, which is upthrown to the east, the footwall faults have been termed backthrusts (Sterne, 2006). The anomalous younger-over-older contractional fault relationships in Garden of the Gods, other localities in the Front Range (Sterne, 2006), and other sites worldwide have of late been explained by a modified triangle zone model, wherein a wedge bounded by floor and roof thrusts undergo internal deformation (Fig. 10) to accommodate an intensification of strain. In this scheme, the Rampart Range fault is interpreted as a late foreland-directed "piercement" thrust that cuts upsection through all preexisting structures. Our field observations are compatible with the evolved triangle zone model. However, the two-dimensional solution of Sterne (2006) for the comparatively small structural domain of Garden of the Gods has yet to be applied in three dimensions and at the scale of the Rampart Range, which would afford the possibility to address the out-of-plane (strike and oblique slip) displacements that are prevalent there. During this field trip, the faults will be examined from a process standpoint, because they offer an arrested view of brittle deformation that appears to accommodate "room problems" arising from Rampart Range fault curvature and northward increase in displacement at this location (Morgan et al., 2002).

Brittle faults—description. Distinguishing features of the brittle faults in Garden of the Gods (S.A.F Smith, 2013, personal commun.) are that (1) they are segmented into bedding- parallel and bedding-oblique portions (Figs. 12 and 13); (2) they exhibit strong curvature upon "segment bends," or fault surfaces linking the segments; and (3) the curved linking faults exist within (a) overlap zones of intense wall-rock fracturing (e.g., Childs et al., 2009) or (b) systems of penetrative cataclastic deformation bands (e.g., Fossen et al., 2007). Furthermore, (4) the faults exhibit brittle kinematic criteria indicative not only of reverse- but strike- to oblique-sense of motion (Morgan et al., 2002). Consistently, the bedding-parallel fault segments dip steeply to the east, and

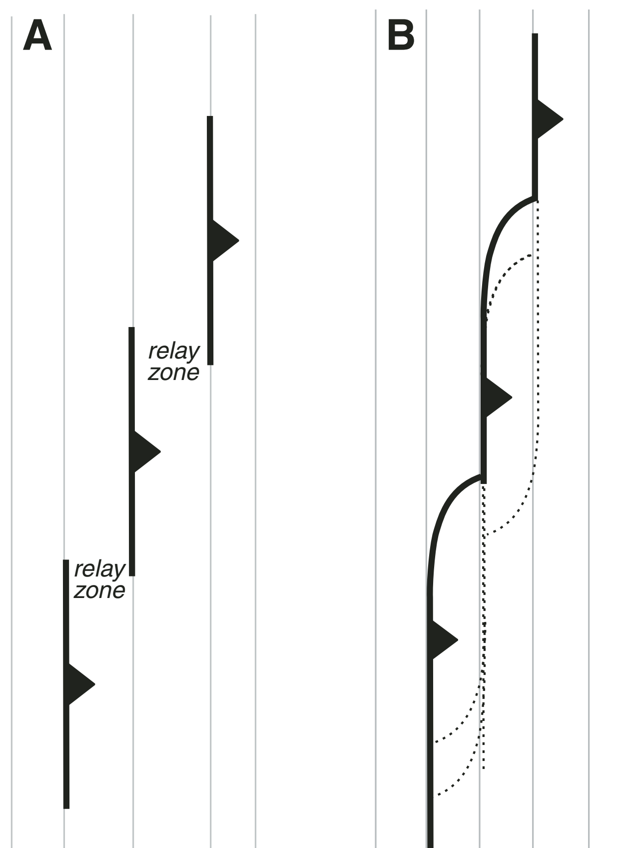

Figure 13. Schematic drawing of structural relay development in clastic units with subvertical bedding. (A) En echelon reverse faults accommodate slip upon bedding in Lyons and Fountain Formations. The zones of overlap between faults are relays subject to brittle deformation. (B) With increased displacement, faults breach the relay zones and link the en echelon segments. The result is a segmented fault with alternating straight and curved segments. Close-spaced shear fractures or deformation bands pervade the fault relay zones.

bedding-oblique fault segments dip steeply to moderately SE. Both are well striated, with compatible kinematics indicative of east-west to NE-SW sense of shear (Morgan et al., 2002). The segment bends that link them display drastic changes in fault strike of up to 90° (Figs. 12 and 13), resulting in a fault geometry that is highly angular in appearance. The wall-rock volume surrounding the segment bends is intensely fractured, with densities up to or exceeding 50 fractures per meter. Within lower Lyons Sandstone, the majority of fractures are shear fractures with well-developed slickenlines recording broadly east-west to NE-SW slip, albeit with small displacement of a few centimeters or less. In the upper Lyons Sandstone, cataclastic deformation bands are prominent as individual structures or as thick clusters dipping to the southeast; individual bands commonly show delicate striae and small offset, and clusters generally are bordered by through-going slip surfaces that host striae (shear fractures or mesoscopic faults).

Structural interpretations. The presence of curved faults within highly fractured overlap zones suggests that the overlaps functioned as fault *relays* that transferred slip from one fault segment to the next (Childs et al., 2009). The prevalence of shear fractures in lower Lyons Sandstone indicates frictional sliding as the dominant failure mechanism within relay zones in that unit, whereas the abundance of deformation bands in the upper Lyons Sandstone reflects grain fracturing + sliding with compaction and permeability loss as the failure mode. With only small slip upon shear fractures, the amount of strain accommodated by lower Lyons fracture networks overall was low. In upper Lyons Sandstone, the pervasive deformation bands and thick deformation band clusters (e.g., Fossen et al., 2007) reflect higher strain accommodated by compaction-induced loss in porosity. The higher porosity of the upper Lyons Sandstone, which led to the preferential development of deformation bands rather than shear fractures, likely was a consequence of hydrocarbon migration (e.g., Higley and Cox, 2007) through the unit. Hydrocarbons create reducing chemical conditions that diminish hematite cement and enhance porosity (Surdam et al., 1993; Lee and Bethke, 1994).

In both units, complex penetrative deformation gave way to slip upon single, through-going shear surfaces or fault strands that effectively breached the relay zones and minimized the surface area of active-slip planes, allowing efficient slip displacement and strain accommodation. The slip surfaces are oriented NE-SW, with dip to SE, which is subparallel to bedding-oblique fault segments. Thus there is geometrical evidence that distributed oblique faults succeeded the penetratively fractured relay zones, offering an expression of how fault zones evolve and simplify through growth and coalescence of individual active fault strands that have "straighter" overall geometries with lower total surface area (e.g., Childs et al., 2009, and references therein). Ultimately, the complexly fractured and faulted region of Garden of the Gods, within a restraining bend of the Rampart Range fault, was itself abandoned as the higher-order Rampart Range fault and roof thrust became energetically efficient. In this process, the highly segmented backthrusts in the Garden of the Gods, with their complex, highly irregular geometry and a relatively large surface area, were preserved. The intense wall-rock fracturing and reduction of sandstone porosity within deformation bands and clusters were mechanisms that caused faults in the Garden of the Gods to evolve toward a more efficient planar geometry.

QUESTIONS FOR DISCUSSION

The goal of this field trip is to explore persistent geological problems in the Colorado Springs area as a stimulus for discussions about geological processes and events that have broader regional or global significance. We hope that scientific dialogue during the field trip will enhance the general understanding of paleoenvironments that have relevance to global cycles, will acquaint participants with distinctive structures that offer a record of singular events uniquely recorded in Colorado Springs, and will open conversation about the potential interplay of crustal deformation and surface processes in response to climate shifts. We pose the following questions as a starting point for discussion.

- Recently, the global shift in ocean chemistry that was associated with the Cambrian explosion of multicellular life has been linked to the deep, intense chemical weathering associated with the Great Unconformity. What processes were in effect to produce the chemically mature, quartz-rich basal Cambrian strata that rest upon the Great Unconformity? Might these paleoenvironmental factors have arisen at multiple times in the Proterozoic? When detrital zircons with distant provenance are found in Cambrian strata, what does this signify about the span of time represented by the Great Unconformity?
- New data presented during this field trip support the designation of Tava sandstone as distinct from Sawatch Formation sandstone. What is the significance of the observational evidence for contrasting paleoenvironments of formation for each, that bear on the relative age and paleotectonic and/or paleogeographical context for the sandstones?
- Geological elements of the Front Range embayment point to a tectonically active environment in early Paleozoic time or prior. There is evidence of glauconitic tidal dunes, purported hyperconcentrated flows and injectites, and geophysical anomalies. Is there a unifying tectonic framework that can accommodate the disparate pieces of evidence and constrain the time interval?
- The catalog of detrital zircon records for the western United States is growing, leading to development of characteristic provenance patterns in relative age probability diagrams that can be used to link sedimentary rocks to their sources and narrow down the time of deposition. The results of U-Pb detrital zircon studies on samples gathered along the Ute Pass fault show both broad regional trends suggestive of distant transport and mixing and distinct peaks indicative of local derivation. What accounts for the differences in spectra from samples collected over a comparatively small area? What distinctions may be drawn between

Sawatch Formation and Tava sandstone? What do the results reveal about the extent of exposure of Precambrian rocks, and about tectonic events that caused variable bedrock uplift and unroofing?
- There are contradictory standpoints on the time of deposition of Laramide synorogenic sediments in intermontane basins bordering the Front Range. Drawing upon material covered on the field trip, does $^{40}Ar/^{39}Ar$ illite age analysis offer a potential resolution of the question about precise timing of development of Laramide structures? What is the meaning of the apparent contemporaneity of formation of the Front Range monocline, sedimentation in intermontane basins, and the Paleocene–Eocene Thermal Maximum?
- Fault relays and linkage zones are known from extensional fault systems, but little is known from contractional settings. What accounts for the preservation of the structures at Garden of the Gods, in a contractional setting? Based on field trip observations of meter- to kilometer-scale features in the structural system of Garden of the Gods, is it plausible that the Garden itself represents a comparable but larger-scale zone of complexity, now abandoned, that is a vestige of a stage in the initiation of the southern Rampart Range fault at ca. 57 Ma?

FIELD TRIP ITINERARY

Day 1

Stop 1A: Manitou Avenue, West End

To reach Stop 1, take Highway 24 West from Colorado Springs to Manitou Springs (Fig. 1). Just past mile marker 298, there is a stoplight for Manitou Springs/Cave of the Winds. Go left at the light onto Serpentine Drive, and proceed downhill along Fountain Creek to a stop sign at Manitou Avenue. Take a SHARP right uphill on Manitou Avenue toward Hwy 24 for 0.4 miles. CAREFULLY turn left, crossing the road onto a short dirt road that leads to parking in an abandoned small quarry.

This stop features the Great Unconformity separating the latest Mesoproterozoic Pikes Peak Granite from the Upper Cambrian Sawatch Formation. Here we look at basal deposits of the transgressive Cambrian seaway (Fig. 2), including very large scale, glauconite-rich, tidal subaqueous dunes (heights of several meters and wavelengths of >100 m). We will also see a Cambrian–Ordovician disconformity surface with the overlying Manitou Formation. The disconformity records gentle uplift and erosion during the early Ordovician, with progressive erosional removal of strata to the south. Above the Manitou Formation, thick alluvial fan red-bed deposits of the Fountain Formation record Pennsylvanian Ancestral Rockies uplift.

Stop 1B (Optional): Serpentine Drive, Manitou Springs

Retrace the route for Stop 1 by driving downhill 0.4 mi, taking a sharp left at the first intersection, onto Serpentine Drive. Proceed to hairpin turn and park in the Rainbow Falls parking area.

Immediately upslope from the parking area, there are exposures of the Great Unconformity and Sawatch Formation within the same section as examined at Stop 1. Here the tidal dune deposits contain much more trough cross bedding, which makes up the large-scale foresets. The strata just above the dune deposits may be examined in exposures that are several yards downhill from the parking pullout, on the opposite side of Serpentine Drive, along the creek. Extensive bedding planes contain abundant eocrinoid columnals and bioturbated dolomitic and glauconitic deposits.

Farther downhill, just a short distance along the road, access to exposures of Manitou Limestone may be gained by crossing a dip down into a gulley on the left (east side of the road), just before a bridge, following a small path to a cave. Here the lowermost Manitou Limestone contains well-developed, upward-shoaling, meter-scale peritidal cycles (Myrow, 1995; Fig. 5). Cycles consist, in ascending order, of (1) a basal wave-rippled grainstone; (2) thin, ribbon-bedded micrite; (3) very thin to thin, nodular-bedded micrite; (4) *Thalassinoides*-bioturbated micrite; and (5) a planar hardground surface. The shoaling nature of these cycles is reflected in the transition from coarse-grained grainstone to micrite, an upward thinning of bedding both within the ribbon beds and between the ribbon and nodular beds, and evidence for subaerial exposure—microkarst and pseudomorphs of evaporite minerals—in the burrowed intervals below hardground surfaces. Myrow (1995) described a new species of the trace fossil *Thalassinoides* from these strata. *Thalassinoides* is most abundant in the nodular-bedded and bioturbated sub-hardground micritic lithofacies in the upper parts of these cycles (Fig. 5) that reflect an upward transition from soft sediment to firmground to hardground conditions.

The planar hardground surfaces contain truncated marcasite nodules that formed during early diagenesis and were planed off with the rest of the hardground during subsequent relative sea level rise. The overlying grainstone apparently abraded these hardground deposits as the grains were reworked by waves. This reworking formed surficial lags of large gastropods and trilobite spines on the upper surfaces of the wave ripples.

Stop 2: 96-Foot Bridge, Canon Avenue, Manitou Springs

Stop 2 focuses upon exposures of paleokarst carbonate of the Mississippian Hardscrabble Formation (Leadville Limestone; see above), followed by a walk to Stop 2b, the marginal marine deposits of the Glen Eyrie Shale basal member of the Fountain Formation.

To arrive at Stop 2, drive downhill into downtown Manitou Springs. Continue through and past the roundabout for ~300 m and take a sharp left onto Canon Avenue at a small intersection island. Continue for ~250 m, making a right turn after passing the historic Cliff House hotel. This is the continuation of Canon Avenue. Proceed ~300 m and bear left staying on Canon Avenue. Go under the Highway 24 bridge and park on side of road. To reach Stop 2b, continue on foot up the road to a very sharp hairpin, where there is an historic sign marking the exit to Cave of the Winds. Make the turn and continue steeply uphill for ~150 m.

In road cuts on the left, note the blocky disrupted karst collapse breccia and fault breccia associated with a high-angle fault (Keller et al., 2005). The road bends to the left, and just beyond the first house (on the right), walk into a gulley on the left side of the road. Visitors to this site are advised to park beneath the bridge and walk (rather than drive) to Stop 2b because there is little/no parking nor turnaround space for vehicles at the top of the road that leads to a dead end and private residences.

Exposures bordering the bridge abutments for Highway 24 display medium-bedded, partially dolomitized (brown color) carbonate mudstone that lacks macrofauna. Several small to large pockets of paleokarst collapse breccia are well displayed, particularly on the left side of the outcrop. The outcrop shows slight folding of tilted layers. Clasts are subangular to angular and consist of carbonate mudstone of similar composition and texture to the host rock. The paleokarst breccia records exposure and the formation of karst caves by dissolution under meteoric water beneath the unconformity surface with overlying Glen Eyrie Shale Member of the Pennsylvanian Fountain Formation. The sharp stratigraphic transition to the Glen Eyrie is examined at Stop 2b.

Stop 2b visits the lower Fountain Formation (Glen Eyrie Member) at a site with large displaced blocks of quartz sandstone on the floor and right-hand wall of the gulley. The strata consist of organic-rich shale, siltstone, and sandstone. The thin to medium sandstone beds are well lithified and are the source of the fallen slabs that contain circular plant trace fossils of *Lepidodendron*, a common Carboniferous spore-bearing plant, upon bedding surfaces. Above a ledge in the gulley is a large block (~1 m across) of sandstone that contains a spectacular *Lepidodendron* fossil of an anchoring *Stigmaria* (root-like) structure. The root-like feature shows the characteristic diamond-shaped, bark-like surface and slender, remarkably well preserved tapering projections. These projections may have acted more like leaves than roots, and given the shallow burial of the *Stigmaria*, they may have projected above the surface and been capable of photosynthesis.

The slab containing the fossil was eroded directly from the gulley wall that exposes the Glen Eyrie member. We suspect that the circular traces were produced by penetration of growing projections, similar to those preserved on the *Stigmaria* fossil on the large slab.

New detrital zircon provenance data for quartz sandstone within the Glen Eyrie Shale will be displayed at this stop (Siddoway, unpublished), for insight about possible locations of incipient uplift that may have been responsible for the regression. The new U-Pb isotope data show an abundance of 1.72 and 1.48 Ga zircons, with a virtual absence of 1.08 Ga zircon that would signify the exposure and erosion of Pikes Peak Granite (Fig. 9).

Stop 3: Intemann Nature Trail Trailhead, Crystal Park Road, Manitou Springs

Leaving Stop 2, retrace the route back to Manitou Avenue via Canon Avenue and a one-way segment of Park Avenue. At the stoplight, turn left on Manitou Avenue and proceed 1.2 miles east to the stoplight at Crystal Park Road: turn right. Drive on Crystal Park Road to the entrance booth for the Crystal Park gated community; turn around and backtrack 0.2 miles to a pullout on right side of road, where there is an access point to the Intemann Nature Trail (www.intemann-trail.com/Maps/Cemetery.png). Disembark and get on the trail on the west side of the road, walk 0.3 miles to off-trail exposures of a heretofore unnamed and undescribed sandstone that is bounded by faults above and below.

At this location, we will examine a fault-bounded sandstone body (Fig. 14) and two generations of sandstone injectites in scattered exposures along the middle elevations of the hill west of Crystal Park Road and Sutherland Creek. The site presents an optimal location to observe primary features and discuss long-standing controversies about the origin and age of the tabular sandstone bodies and dikes. Along its length, the Intemann Nature Trail traverses many sandstone dikes within brittle sheared granite within the hanging wall of the Ute Pass fault.

The Sutherland Creek sandstone (Fig. 14A) has a lateral extent of ~1 km and thickness of ~40 m; however, the original dimensions of the sandstone body are not known because the sandstone is bounded above and below by low-angle faults (Fig. 14B). The quartz sandstone is massive, with dispersed, non-touching granules and pebbles of quartz, and occasional flakes of mudstone (Figs. 6 and 7). Indistinct, unbounded cross beds and discontinuous subhorizontal parallel lamination may be found within the largely structureless, massive sandstone. The material is diffusely graded in respect to matrix grain size and dispersed class size in some areas. The sandstone structurally overlies moderately inclined Fountain Formation and is structurally overlain by Proterozoic metamorphic rocks and granite (Fig. 14A).

Light-colored, well-indurated sandstone sills, with delicate apophyses, cut the massive sandstone, which is deep red with pervasive reduction spots and mottling. One sill closely follows the fault contact at the top of the massive sandstone, with thin apophyses that project a short distance from the sill into the gneiss and granite of the hanging wall. The sill passes upward into one or more sandstone dikes hosted by Proterozoic gneiss, schist, and granite. Crosscutting relationships show that at least two generations of dikes intruded the crystalline unit (Fig. 15). Despite a structural overprint by minor faults and brittle shears, there is near-continuity between sandstone-hosted dikes and crystalline-hosted dikes, a relationship that has not been discovered at any other massive sandstone location. Sedimentological and petrographic similarities between sand body and dikes indicate that the massive sandstone is a plausible source of material for the dikes; however, the crosscutting relationships with evidence of multiple intrusion events suggest that the dikes originated from parent material that was deeper or at some lateral distance to the section. Anisotropy of magnetic susceptibility (AMS) characteristics of the sandstone dikes provides evidence that the dikes formed as injectites with a high energy of emplacement (Freedman, 2013) rather than by

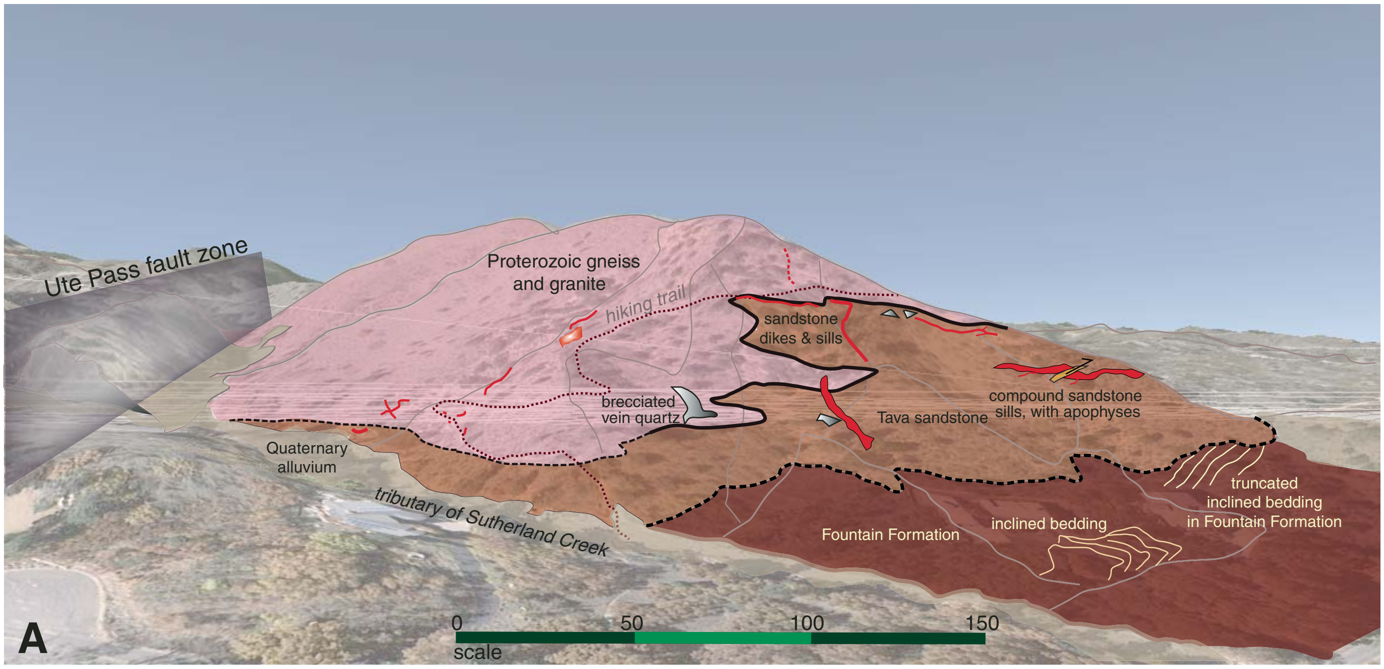

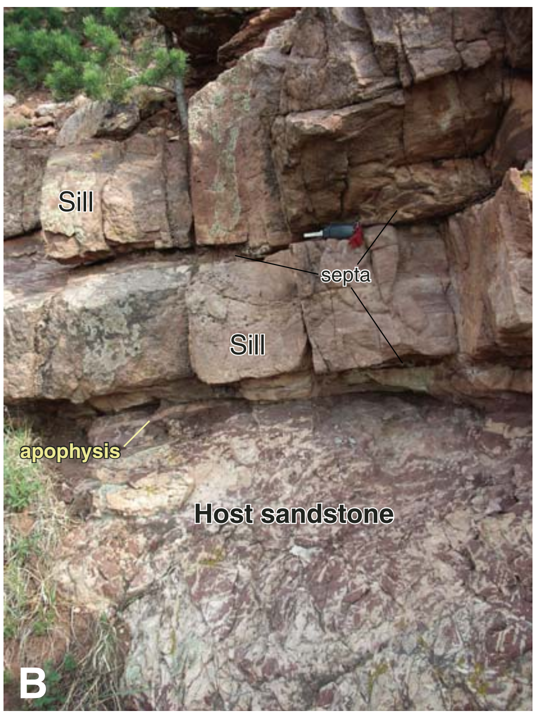

Figure 14. (A) Sketch illustrating structural context of “Tava sandstone” body at Sutherland Creek (Stop 3). The close spatial association of sandstone-hosted sills and gneiss-hosted dikes may indicate that the upper volume of Proterozoic rock was emplaced as an olistolith; that is, a gravity slide block translated onto the Tava sandstone body that is representative of the “parent” sands. View is to the north-northwest. Vertical exaggeration is 2×. (B) Photo of massive Tava sandstone body that is cut by sandstone sills and dikes. The sandstone body is bounded by low-angle faults that separate the massive sandstone from moderately dipping Fountain Formation, below, and Proterozoic gneiss and granite, above. A laterally continuous sill, 0.5–1 m thick, intruded the upper fault contact, and apophyses from the sill pass upward across the fault into Proterozoic gneiss of the hanging wall. The close spatial association of sandstone-hosted sills and gneiss-hosted dikes may indicate that the upper volume of Proterozoic rock was emplaced as an olistolith; that is, a gravity slide block translated onto the Tava sandstone body. (C) Panoramic photo and sketch that illustrate the extent and location of through-going sandstone dikes along the Ute Pass fault zone (UPF) across Cheyenne Cañon and below Mount Cutler. Width of image is 0.9 km.

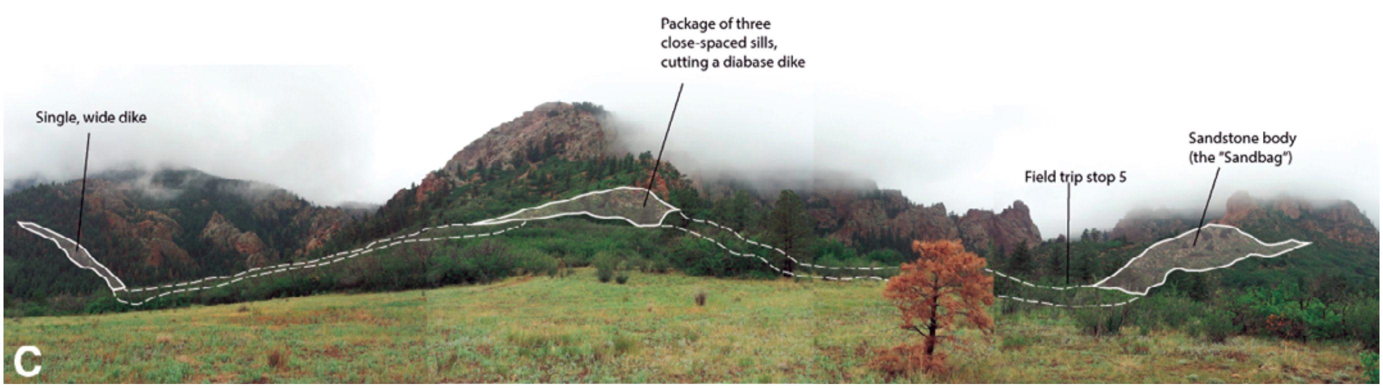

Figure 15. Photo of crosscutting sandstone dikes within Proterozoic granite, Sutherland Creek sandstone body. One dike is parallel to a pronounced brittle fracture cleavage in the granite, and the other cuts across it. Length of scale card: 15 cm. Photo: Matt Rosales.

a process of gravitational infilling (Harms, 1965; c.f. Dockal, 2005). Aligned granule or pebble lenses and fine-scale lamination parallel to dike margins (rare at the localities here reported) support that interpretation.

Stop 4: Overlook, Manitou Springs High School

Return back down Crystal Park Road to Poplar Place/Santa Fe Place, where the street makes a 90° bend to the right, just before Manitou Ave. Turn left, following the indication on a small sign for Manitou Springs High School. Ascend Santa Fe Place to the high school entrance, veering right to go around the main building to the parking lot behind. Walk to the site of a small monument on a round concrete pad, where there is a good vantage point for the Manitou Springs embayment. [NOTE: Unaccompanied visitors to the school should stop briefly in Visitor Parking by the main entrance, and check in at the front desk to request permission to view geology on the premises.]

In view to the northwest and north are the Ute Pass fault, Front Range monocline, and Rampart Range fault in profile at the Garden of the Gods. The tilted Paleozoic–Mesozoic stratigraphic succession is visible along Fountain Creek/Highway 24 and the thickness of Pennsylvanian Fountain Formation accumulated in a fault-controlled basin during the Ancestral Rocky Mountains orogeny (Suttner et al., 1984; Sweet and Soreghan, 2010) is evident. Exposures of Fountain Formation boulder conglomerate can be studied at the back of the high school parking lot. The large clast size (20–85 cm) indicates that this part of the unit is proximal to source, and abundant boulders of gneiss and schist can be tied to a source in the vestigial thrust block (Keller et al., 2005) that structurally overlies the massive Tava sandstone body visited at Stop 3. Elsewhere in the Fountain Formation, the dominant clast source is Pikes Peak Granite.

Day 2

Stop 5: North Cheyenne Cañon

Diabase and sandstone dikes within Proterozoic crystalline host rock, in road cut along North Cheyenne Cañon Road. Brittle structures of the basement.

To arrive at Stop 5 from downtown Manitou Springs, go west on Manitou Avenue to Serpentine Drive, then uphill to the intersection with U.S. Hwy 24, where there is a stoplight. Turn east onto U.S. Hwy 24 and travel for 4.0 miles to South 21st St.; turn right at stoplight. Drive south on 21st St. for 1.4 miles, where 21st Street becomes Cresta Avenue. Continue straight on Cresta for another 1.6 miles; then turn right on Cheyenne Boulevard for 1 mile. Turn right again on North Cheyenne Cañon Road, where there is a sign noting the entrance to North Cheyenne Cañon Park. Go one mile, passing a small parking lot near a large green water tank on the right side of the road. After a sharp bend to the right on a narrow section of road, carefully pull off in the pullout bordering North Cheyenne Creek on the left side of the road, and park next to a small stone bridge and a large boulder used for sport climbing. Taking care for oncoming traffic, walk back down the paved road to exposures of sandstone dikes just beyond the sharp bend. In addition to the road cut, time is allocated for small groups to undertake short, vigorous, off-trail hikes on steep vegetated terrain to additional nearby outcrops (bushwhacks).

At this stop, the long road cut displays an alternation of granite, diabase, and wide sandstone dikes. Although the outcrop is fractured and weathered, the constituent sandstone and dike contacts can be examined for comparison with observations at Stop 4 on Day 1. The sandstone dikes are hosted by Proterozoic gneiss and granodiorite. They form the north end of a parallel array of southward-narrowing dikes that extends at least 6 km (up to the limit of access at the North American Aerospace Defense Command [NORAD] facility boundary). Whereas a nearby sandstone body consists of well-indurated, structureless, fine-grained sand that *lacks* quartz granules and contains rounded pebbles, the dikes contain matrix-supported, dispersed rounded to angular granules of quartz or feldspar, together with sparse larger fragments of host rock. At Cheyenne Cañon, the color of the massive sandstone and dike rock is dark gray to greenish gray due to presence of chlorite and clay alteration, with red-brown oxidation upon weathered surfaces. There is only minimal development of the red and white color mottling that is widespread elsewhere. An effort to determine the U-Pb titanite or zircon age of the diabase dikes, that could tighten the maximum age limit on Tava sandstone, has so far been unsuccessful.

Other structures in evidence at the mouth of Cheyenne Cañon are large brittle faults and fracture arrays within the Pikes Peak Granite in the hanging wall of the Ute Pass fault. Walking trails on both sides of the creek offer access to the lower parts of the structures. Discussion at this stop will include an overview of the reverse fault segment of the Ute Pass fault at Cheyenne Mountain and geometry and kinematics of the planar brittle structures.

Stop 6: Ridge Road, South Garden of the Gods

Return to U.S. Hwy 24 via Cresta Ave. and 21st Street. Turn west on Hwy 24 for 1 mile, then turn right on S 31st St. Take the first left onto W. Colorado Ave., then drive 0.6 miles to Ridge Rd. Turn right and go 0.6 miles to enter Garden of the Gods Park (Fig. 12) from the south. Pull off to the left into the parking area for a scenic overlook.

This stop offers a vantage point for the Ute Pass and Rampart faults and views to north and south along the steep limb of the Front Range monocline. Discussion will focus upon the Laramide structure of the Front Range, structural inheritance, the timing of Laramide tectonism, and relation to tectonic sedimentation.

Stop 7: Garden of the Gods Park

From the overlook, drive north a short distance to Juniper Way Loop road; turn right and circumnavigate the narrow monoliths that form the Garden of the Gods. Pass the juncture with Garden Drive, which goes off to the west. Continue south a short distance, pull into the first small parking lot on the right, and disembark.

The focus of this stop is complex deformation within the sandstones and conglomerates forming the footwall of the Rampart Range fault (Figs. 10 and 12), which has led to development of mesoscopic structures with unusual attributes. The Garden of the Gods offers three-dimensional access to complex, steep, younger-upon-older reverse faults, domains with a high density of deformation bands, and unusual curved dihedral faults (Fig. 13) that offer rare examples of fault linkage zones in a contractional setting.

At this stop, short guided walks lead to three sites of structural interest: (1) The Hidden Inn fault provides a site for discussion of new results from $^{40}Ar/^{39}Ar$ illite age analysis of fault-gouge, involving sophisticated methods for mineral separation and clay mineral characterization. (2) The Gateway Rock provides an exposure of the transitional contact between Fountain Formation and Lyons Formation, with bedding cut and displaced by lovely conjugate fractures and faults. (3) In Lyons Sandstone at the north end of "Red Fin" monolith, it is possible to examine segmented, stepped faults over a range of scales from a few tens of centimeters to tens of meters; deformation band systems; and zones of wall-rock fracturing, as per the descriptions provided above.

ACKNOWLEDGMENTS

Warm thanks are due to collaborators Mike Petronis, Arlo Weil, Steven A.F. Smith, and Jay Temple. Colorado College student researchers contributed to the new progress on the structural geology problems examined on this field trip, with individual thanks to: Lizzy Fay, Matt Rosales, Ashley Contreras, David Freedman, Hannah Karlsson, and Sally Shatford. Acquaintance with some key exposures was obtained through work supported by the Colorado Geological Survey, during a period of rich geological discovery brought about by the survey's quadrangle mapping program. Two canines, Pearl and Bessie, are responsible for off-trail hikes that led to discovery of numerous new dike localities. Conversations with George Gehrels, Henry Fricke, Chris Hall, and Ben van der Pluijm helped to solidify the hypotheses arising from preliminary isotopic data. Isotopic data for geochronology were obtained at the University of Arizona Laserchron Center and University of Michigan Argon Geochronology Laboratory, with the aid of able staff. We acknowledge land access granted by the Louisiana State University field camp, Castle Concrete Company (Mac Shafer), and Colorado Springs Parks, Recreation, and Cultural Services. Colorado College provided institutional research funds and covered the costs of vehicle use on the GSA field trip. Sincere thanks go to Karen Houck, Jay Temple, Jeff Noblett, and Lon Abbott for critical reviews of this field trip guide. We're grateful to Lon Abbott and Greg Hancock, the editors of the 2013 GSA field guide volume, for their vision and hard work.

REFERENCES CITED

Allen, G.P., and Posamentier, H.W., 1993, Sequence stratigraphy and facies model of an incised valley fill: The Gironde Estuary, France: Journal of Sedimentary Petrology, v. 63, p. 378–391.

Allen, J.L., 1994, Stratigraphic variations, fault rocks, and tectonics associated with brittle reactivation of the Homestake Shear Zone, central Colorado [Ph.D. thesis]: University of Kentucky, 296 p.

Allen, J.R.L., 1980, Sand waves: A model of origin and internal structure: Sedimentary Geology, v. 26, p. 281–328, doi:10.1016/0037-0738(80)90022-6.

Amato, J.M., and Mack, G.H., 2012, Detrital zircon geochronology from the Cambrian–Ordovician Bliss Sandstone, New Mexico: Evidence for contrasting Grenville-age and Cambrian sources on opposite sides of the Transcontinental Arch: Geological Society of America Bulletin, v. 124, p. 1826–1840, doi:10.1130/B30657.1.

Berg, R.R., and Ross, R.J., Jr., 1959, Trilobites from the Peerless and Manitou formations, Colorado: Journal of Paleontology, v. 33, p. 106–119.

Bird, P., 1988, Formation of the Rocky Mountains, Western United States: A Continuum Computer Model: Science, v. 239, p. 1501–1507, doi:10.1126/science.239.4847.1501.

Brasier, M.D., 1980, The Lower Cambrian transgression and glauconite-phosphate facies in western Europe: Journal of the Geological Society [London], v. 137, p. 695–703, doi:10.1144/gsjgs.137.6.0695.

Cartwright, J., 2010, Regionally extensive emplacement of sandstone intrusions: A brief review: Basin Research, v. 22, no. 4, p. 502–516, doi:10.1111/j.1365-2117.2009.00455.x.

Cattaneo, A., and Steel, R.J., 2003, Transgressive deposits: A review of their variability: Earth-Science Reviews, v. 62, p. 187–228, doi:10.1016/S0012-8252(02)00134-4.

Childs, C., Manzocchi, T., Walsh, J.J., Bonson, C.G., Nicol, A., and Schopfer, M.P.J., 2009, A geometric model of fault zone and fault rock thickness variations: Journal of Structural Geology, v. 31, p. 117–127, doi:10.1016/j.jsg.2008.08.009.

Chronic, J., and Williams, C.A., 1978, The Glen Eyrie Formation (Carboniferous) near Colorado Springs: Rocky Mountain Association of Geologists Symposium, p. 199–206.

Crosby, W. O., 1897, Sandstone dikes accompanying the great fault of Ute Pass, Colorado: Science, v. 5, no. 120, p. 604–607.

Cross, W., 1894, Intrusive sandstone dikes in granite: Geological Society of America Bulletin, v. 5, p. 225–230.

Davis, R.A., Jr., Klay, J., and Jewell, P., IV, 1993, Sedimentology and stratigraphy of tidal sand ridges southwest Florida inner shelf: Journal of Sedimentary Petrology, v. 63, p. 91–104.

Dockal, J.A., 2005, Sandstone 'dikes' within the Arapaho Pass Fault, Indian Peaks Wilderness, Boulder and Grand counties, Colorado: The Mountain Geologist, v. 42, p. 143–158.

Dulin, S.A., and Elmore, R.D., 2013, Clastic dikes within the Pikes Peak Granite of the Front Range, Colorado: Using paleomagnetism to constrain age of emplacement: Geological Society of America Abstracts with Programs, v. 45, no. 7, paper no. 361-2.

Duller, R.A., Mountney, N.P., and Russell, A.J., 2010, Particle fabric and sedimentation of structureless sand, southern Iceland: Journal of Sedimentary Research, v. 80, p. 562–577, doi:10.2110/jsr.2010.055.

Erslev, E.A., Holdaway, S.M., O'Meara, S., Jurista, B., and Selvig, B., 2004, Laramide minor faulting in the Colorado Front Range, *in* Cather, S.M., McIntosh, W.C., and Kelley, S.A., eds., Tectonics, Geochronology, and Volcanism in the Southern Rocky Mountains and Rio Grande Rift: New Mexico Bureau of Geology and Mineral Resources Bulletin, v. 160, p. 181–204.

Ethington, R.L., and Clark, D.L., 1981, Lower and Middle Ordovician conodonts from the Ibex area, western Millard County, Utah: Brigham Young University Studies, v. 28, pt. 2, 155 p.

Fay, E., and Siddoway, C., 2004, Insights on the kinematic evolution of the Ute Pass fault zone from investigation of mesoscopic brittle faults: Geological Society of America, Abstracts with Programs, v. 36, no. 5, Abstract No. 78370.

Fenster, M.S., Fitzgerald, D.M., Bohlen, W.F., Lewis, R.S., and Baldwin, C.T., 1990, Stability of giant sand waves in eastern Long Island Sound, U.S.A: Marine Geology, v. 91, p. 207–225, doi:10.1016/0025-3227(90)90037-K.

Finlay, G.I., 1907, The Glen Eyrie formation and its bearing on the age of the Fountain Formation in the Manitou region, Colorado: The Journal of Geology, v. 15, p. 586–589, doi:10.1086/621430.

Finlay, G.I., 1916, Geologic Atlas of the United States: Colorado Springs Folio, Colorado: U.S. Geological Survey Folio 203, scale 1:25,000, 5 sheets, 15 p. text.

Fisher, L.R., and Fisher, T.R., 2004, Continental accretion, Colorado style: Proterozoic island arcs and backarcs of the Central Front Range: Geological Society of America Field Guides 2004, v. 5, p. 109–129, doi:10.1130/0-8137-0005-1.109.

Fitz-Díaz, E., and van der Pluijm, B., 2013, Fold dating: A new approach to constrain the age of shortening in shallow crustal rocks: Journal of Structural Geology, doi:10.1016/j.jsg.2013.05.011 (in press).

Foland, K., Hubacher, F.A., and Arehart, G.B., 1992, ^{40}Ar/^{39}Ar dating of fine grained samples: An encapsulated-vial procedure to overcome the problem of ^{39}Ar recoil loss: Chemical Geology, v. 102, p. 269–276, doi:10.1016/0009-2541(92)90161-W.

Fossen, H., Schultz, R.A., Shipton, Z.K., and Mair, K., 2007, Deformation bands in sandstone: A review: Journal of the Geological Society [London], v. 164, p. 755–769, doi:10.1144/0016-76492006-036.

Freedman, D., 2013, Paleomagnetism and anisotropy of magnetic susceptibility of clastic dikes of the Colorado Front Range: Determination of Age and Origin [B.A. thesis]: Colorado Springs, The Colorado College, 73 p.

Freedman, D., Petronis, M.S., and Siddoway, C.S., 2012, Geomagnetic Investigation of Sandstone Dikes of the Colorado Front Range, for Determination of Age and Mode of Emplacement: San Francisco, California, American Geophysical Union, 2012 Fall Meeting, abstract GP21A-1132.

Frey, R.W., and Seilacher, A., 1980, Uniformity in marine invertebrate ichnology: Lethaia, v. 13, p. 183–207, doi:10.1111/j.1502-3931.1980.tb00632.x.

Fricke, H.C., Kochevar, E., Clyde, W.C., Snell, K.E., Martin, K., and Miller, I., 2012, Landscape change and megafan deposition in the Denver Basin during the PETM: San Francisco, California, American Geophysical Union, 2012 Fall Meeting, abstract T13F-2466.

Geissman, J., and Harlan, S., 2002, Late Paleozoic remagnetization of Precambrian crystalline rocks along the Precambrian/Carboniferous nonconformity, Rocky Mountains: A relationship among deformation, remagnetization, and fluid migration: Earth and Planetary Science Letters, v. 203, p. 905–924, doi:10.1016/S0012-821X(02)00932-9.

Gerhard, L.C., 1972, Canadian depositional environments and paleotectonics, central Colorado, *in* De Voto, R.H., ed., Paleozoic Stratigraphy and Structural Evolution of Colorado: Colorado School of Mines Quarterly, v. 67, no. 4, p. 1–36.

Gruszka, B., and Zieliński, T., 1966, Gravity flow origin of glaciolacustrine sediments in a tectonically active basin: Annales Societatas Geologorom Poloniae, v. 66, p. 59–81.

Haines, S., and van der Pluijm, B., 2008, Clay quantification and Ar dating of synthetic and natural gouge: Application to the Miocene Sierra Mazatlán detachment fault, Sonora, Mexico: Journal of Structural Geology, v. 30, p. 525–538, doi:10.1016/j.jsg.2007.11.012.

Hamilton, W.B., and Myers, W.B., 1966, Cenozoic tectonics of the western United States: Reviews of Geophysics, v. 4, p. 509–549, doi:10.1029/RG004i004p00509.

Harms, J., 1965, Sandstone dikes in relation to Laramide faults and stress distribution in the southern Front Range, Colorado: Geological Society of America Bulletin, v. 76, p. 981–1001, doi:10.1130/0016-7606(1965)76[981:SDIRTL]2.0.CO;2.

Higley, D.K., and Cox, D.O., 2007, Oil and Gas Exploration and Development, Denver Basin, Colorado, Nebraska, and Wyoming, *in* Higley, D.K., compiler, Petroleum Systems and Assessment of Undiscovered Oil and Gas in the Denver Basin Province, Colorado, Kansas, Nebraska, South Dakota, and Wyoming—USGS Province 39: U.S. Geological Survey Digital Data Series DDS-69-P, Ch. 2, 41 p.

Hill, V.S., 1983, Mississippian Williams Canyon Limestone, member of the Leadville Limestone, central Colorado [M.S. thesis]: Golden, Colorado School of Mines, 101 p.

Hine, A.C., 1977, Lily Bank, Bahamas: History of an active oolite sand shoal: Journal of Sedimentary Petrology, v. 47, p. 1554–1581.

Hoesch, W.A., 2008, Sandstone dikes of the Colorado Front Range and their relation to petroleum exploration in the adjacent Denver Basin: Proceedings—Subsurface Sediment Remobilization and Fluid Flow in Sedimentary Basins (21–28 October 2008) [abs.]: The Geological Society of London, p. 107.

Houbolt, J.J.H.C., 1982, A comparison of recent shallow marine tidal sand ridges with Miocene sand ridges in Belgium, *in* Scrutton, R.A., and Talwani, M., eds., The Ocean Floor: New York, John Wiley and Sons, Ltd., p. 69–80.

Houck, K.J., Funk, J.A., Kirkham, R.M., Carroll, C.J., and Heberton-Morimoto, A.D., 2012, Marmot Peak Quadrangle, Park and Chaffee Counties, Colorado: Colorado Geological Survey, scale 1:24,000, http://geosurveystore.state.co.us/p-1425-marmot-peak-quadrangle-park-and-chaffee-counties-colorado.aspx.

Hurst, A., and Glennie, K., 2008, Mass-wasting of ancient aeolian dunes and sand fluidization during a period of global warming and inferred brief high precipitation: The Hopeman Sandstone (late Permian), Scotland: Terra Nova, v. 20, p. 274–279, doi:10.1111/j.1365-3121.2008.00817.x.

Hurst, A., Scott, A., and Vigorito, M., 2011, Physical characteristics of sand injectites: Earth-Science Reviews, v. 106, p. 215–246, doi:10.1016/j.earscirev.2011.02.004.

Jennings, J.R., 1980, Fossil plants from the Fountain Formation (Pennsylvanian) of Colorado: Journal of Paleontology, v. 54, p. 149–158.

Jolly, R.J.H., and Lonergan, L., 2002, Mechanisms and controls on the formation of sand intrusions: Journal of the Geological Society [London], v. 159, p. 605–617, doi:10.1144/0016-764902-025.

Jones, P.B., 1996, Triangle zone geometry, terminology and kinematics, in MacKay, P.A., Varsek, J.L., Kubli, T.E., Dechesne, R.G., Newson, A.C., and Reid, J.P., eds., Triangle zones and tectonic wedges: Bulletin of Canadian Petroleum Geology, v. 44, no. 2, p. 139–152.

Jones, J.V., III, Connelly, J.N., Karlstrom, K.E., Williams, M.L., and Doe, M.F., 2009, Age, provenance, and tectonic setting of Paleoproterozoic quartzite successions in the southwestern United States: Geological Society of America Bulletin, v. 121, p. 247–264, doi:10.1130/B26351.1.

Karlsson, H., Fitz Diaz, E., Siddoway, C.S., and Hall, C., 2013, Ar-Ar illite geochronology for dating of fault and fold deformation in the Front Range monocline, Colorado Springs region: Geological Society of America Abstracts with Programs, v. 45, no. 7, paper no. 368-3.

Keller, J.W., Siddoway, C.S., Morgan, M.L., Route, E.E., Grizzell, M.T., Sacerdoti, R., and Stevenson, A., 2005, Geologic map of the Manitou Springs 7.5-minute quadrangle, El Paso and Teller Counties, Colorado: Colorado Geological Survey Open-File Report 03-19, scale 1:24,000, 41 p.

Kirkham, R.M., Houck, K.J., Funk, J., Mendel, D., and Sicard, K.R., 2012, Minturn Quadrangle, Eagle County, Colorado: Colorado Geological Survey, scale 1:24,000, http://geosurveystore.state.co.us/p-1377-minturn-quadrangle-eagle-county-colorado.aspx.

Kluth, C.F., and Nelson, S.N., 1988, Age of the Dawson Arkose, Southwestern Air Force Academy, Colorado, and implications for the uplift history of the Front Range: The Mountain Geologist, v. 25, p. 29–35.

Kost, L., 1984 Paleomagnetic and petrographic study of sandstone dikes and the Cambrian Sawatch sandstone, eastern flank of the southern Front Range, Colorado [M.S. thesis]: Boulder, Colorado, University of Colorado, 173 p.

Lee, M.-K., and Bethke, C.M., 1994, Late cementation and petroleum accumulation in the (Permian) Lyons sandstone, Denver basin: American Association of Petroleum Geologists Bulletin, v. 78, p. 217–237.

Le Heron, D.P., and Etienne, J.L., 2005, A complex subglacial clastic dyke swarm, Solheimajokull, southern Iceland: Sedimentary Geology, v. 181, p. 25–37, doi:10.1016/j.sedgeo.2005.06.012.

Leonard, E.M., Hubbard, M.S., Kelley, S.A., Evanoff, E., Siddoway, C.S., Oviatt, C.G., Heizler, M., and Timmons, M., 2002, High Plains to Rio Grande Rift: Late Cenozoic Evolution of Central Colorado, *in* Science at the Highest Level: Geological Society of America, Field Guides 2002, v. 3, p. 59–93.

Lewis, J.H., 1965, Petrology and diagenesis of Upper Cambrian rocks of central and western Colorado [Ph.D. thesis]: Boulder, Colorado, University of Colorado, 184 p.

Ludvigsen, R., and Westrop, S.R., 1985, Three new Upper Cambrian stages for North America: Geology, v. 13, p. 139–143, doi:10.1130/0091-7613(1985)13<139:TNUCSF>2.0.CO;2.

Luiszer, F.G., 1999, Field trip to Manitou Springs, Colorado, with specific emphasis on the sediments of Cave of the Winds and and their relationship to nearby alluvial deposits and spring sediments: Geological Society of America Field Guides, v. 1, p. 61–70.

MacKay, P.A., Varsek, J.L., Kubli, T.E., Dechesne, R.G., Newson, A.C., and Reid, J.P., 1996, Triangle zones and tectonic wedges: an introduction, in MacKay, P.A., Varsek, J.L., Kubli, T.E., Dechesne, R.G., Newson, A.C., and Reid, J.P., eds., Triangle zones and tectonic wedges: Bulletin of Canadian Petroleum Geology, v. 44, no. 2, p. I.1–I.5.

Mahon, K., 1996, The new "York" regression: Application of an improved statistical method to geochemistry: International Geology Review, v. 38, p. 293–303, doi:10.1080/00206819709465336.

McMillan, N.J., and McLemore, V.T., 2004, Cambrian–Ordovician magmatism and extension in New Mexico and Colorado: New Mexico Bureau of Geology and Mineral Resources Bulletin, v. 160, p. 1–11.

Middleton, G.V., and Southard, J.B., 1984, Mechanics of sediment movement (2nd ed.): Society of Economic Paleontologists and Mineralogists, Short Course No. 3, Providence, Rhode Island, 401 p.

Milito, S., 2010, A survey of fossils and geology of Red Rock Canyon Open Space, Colorado Springs, Colorado: The Mountain Geologist, v. 47, p. 1–14.

Morgan, M.L., Siddoway, C.S., Rowley, P.D., Temple, J., Keller, J.W., Archuleta, B.H., and Himmelreich, J.W., Jr., 2002, Geologic Map of the Cascade Quadrangle, El Paso County, Colorado: Denver, Colorado, Colorado Geological Survey Open-File Report 03-18, scale: 1:24,000 and text (http://geosurvey.state.co.us/pubs/gis/mapping.asp).

Mulder, T., and Alexander, J., 2001, The physical character of subaqueous sedimentary density flows and their deposits: Sedimentology, v. 48, p. 269–299, doi:10.1046/j.1365-3091.2001.00360.x.

Murray, M., 1975, Late Precambrian volcanic rocks Keeton Porphyry: The Mountain Geologist, v. 12, p. 137–132.

Myrow, P.M., 1995, *Thalassinoides* and the enigma of early Paleozoic open-framework burrow systems: Palaios, v. 10, p. 58–74, doi:10.2307/3515007.

Myrow, P.M., 1998, Transgressive stratigraphy and depositional framework of Cambrian tidal sand wave deposits, Peerless Formation, central Colorado, *in* Alexander, C., Davis, R., and Henry, J., eds., Clastic Tidal Deposition: Society of Economic Paleontologists and Mineralogists, Special Publication 61, p. 143–154.

Myrow, P.M., Taylor, J.F., Miller, J.F., Ethington, R.L., Ripperdan, R.L., and Allen, J., 2003, Fallen arches: Dispelling myths concerning Cambrian and Ordovician paleogeography of the Rocky Mountain region: Geological Society of America Bulletin, v. 115, no. 6, p. 695–713, doi:10.1130/0016-7606(2003)115<0695:FADMCC>2.0.CO;2.

Noblett, J.B., 2011, A Guide to the Geological History of the Pikes Peak Region, Colorado Springs (2nd ed.): Colorado Springs, Colorado, Colorado College, 43 p.

Noblett, J.B., Cohen, A.S., Leonard, E.M., Loeffler, B.M., and Gevirtzman, D.A., 1987, The Garden of the Gods and basal Phanerozoic nonconformity in and near Colorado Springs, Colorado, *in* Beus, S., ed., Geological Society of America Centennial Field Guide for the Rocky Mountain Section: Boulder, Colorado, Geological Society of America, p. 335–338.

Obradovich, J.D., 2002, Geochronology of Laramide synorogenic strata in the Denver Basin, Colorado: Rocky Mountain Geology, v. 37, p. 165–171.

Odin, G.S., and Fullagar, P.D., 1988, Geological significance of the glaucony facies, *in* Odin, G.S., ed., Green Marine Clays: Developments in Sedimentology: Amsterdam, Elsevier, p. 295–332.

Pardo, J., Keller, G.R., and Holloway, S., 2008, New Observations on the Extent of Cambrian Rifting in Colorado: An Update: Geological Society of America Abstracts with Programs, v. 40, no. 6, p. 545.

Pemberton, S.G., and Frey, R.W., 1985, The *Glossifungites* ichnofacies: Modern examples from the Georgia coast, U.S.A., *in* Curran, H.A., ed., Biogenic Structures: Their Use in Interpreting Depositional Environments: Society of Economic Paleontologists and Mineralogists, Special Publication 35, p. 237–259.

Peters, S.E., and Gaines, R.R., 2012, Formation of the 'Great Unconformity' as a trigger for the Cambrian explosion: Nature, v. 484, p. 363–366, doi:10.1038/nature10969.

Raynolds, R.G., 2002, Upper Cretaceous and Tertiary stratigraphy of the Denver Basin, Colorado: Rocky Mountain Geology, v. 37, p. 111–134.

Reynaud, J.Y., Tessier, B., Proust, J.N., Dalrymple, R., Marsset, T., DeBatist, M., Marsset, T., Bourillet, J.F.M., and Lericolais, G., 1999, Eustatic and hydrodynamic controls on the architecture of a deep shelf sand bank (Celtic Sea): Sedimentology, v. 46, p. 703–721, doi:10.1046/j.1365-3091.1999.00244.x.

Ross, M.R., Hoesch, W.A., Austin, S.A., Whitmore, J.H., and Clarey, T.L., 2010, Garden of the Gods at Colorado Springs: Paleozoic and Mesozoic sedimentation and tectonics, *in* Morgan, L.A., and Quane, S.L., eds., Through the Generations: Geologic and Anthropogenic Field Excursions in the Rocky Mountains from Modern to Ancient: Geological Society of America Field Guide 18, p. 77–93.

Runkel, A.D., Miller, J.F., McKay, R.M., Palmer, A.R., and Taylor, J.F., 2007, High-resolution sequence stratigraphy of lower Paleozoic sheet sandstones in central North America: The role of special conditions of cratonic interiors in development of stratal architecture: Geological Society of America Bulletin, v. 119, p. 860–881, doi:10.1130/B26117.1.

Runkel, A.D., Miller, J.F., McKay, R.M., Palmer, A.R., and Taylor, J.F., 2008, The record of time in cratonic interior strata: does exceptionally slow subsidence necessarily result in exceptionally poor stratigraphic completeness?, *in* Pratt, B.L. and Holmden, C., eds., Dynamics of Epeiric Seas: Geological Association of Canada, Special Paper 48, p. 341–362.

Sanders, R.E., 1999, Age of the Keeton porphyry and clast lithologies within the Pennsylvanian Fountain Formation: Implications for the composition of the upper Pikes Peak batholith, Front Range, Colorado [B.A. thesis]: Colorado Springs, Colorado College, 105 p.

Schleicher, A.M., van der Pluijm, B.A., and Warr, L.N., 2010, Nanocoatings of clay and creep of the San Andreas fault at Parkfield, California: Geology, v. 38, p. 667–670, doi:10.1130/G31091.1.

Schneider Santos, J.O., Hartmann, L.A., McNaughton, N.J., Easton, R.M., Rea, R.G., Potter, P.E., 2002, Sensitive high resolution ion microprobe (SHRIMP) detrital zircon geochronology provides new evidence for a hidden Neoproterozoic foreland basin to the Grenville Orogen in the eastern Midwest, U.S.A.: Canadian Journal of Earth Sciences, v. 39, p. 1505–1515.

Schoene, B., and Bowring, S., 2006, U-Pb systematics of the McClure Mountain syenite: Thermochronological constraints on the age of the on the age of the ^{40}Ar/^{39}Ar standard MMhb: Contributions to Mineralogy and Petrology, v. 151, p. 615–630, doi:10.1007/s00410-006-0077-4.

Scott, G.R., 1963, Bedrock Geology of the Kassler Quadrangle: U.S. Geological Survey Professional Paper 421-B, 123 p.

Scott, G.R., and Wobus, R.A., 1973, Geologic map of Colorado Springs area: U.S. Geological Survey, Map MF-482, scale 1:62,500, 1 sheet.

Shipp, R.C., Weimer, P., and Posamentier, H.W., 2011, Mass-Transport Deposits in Deepwater Settings: Tulsa, Oklahoma, Society of Economic Paleontologists and Mineralogists, Special Publication 96, 527 p.

Siddoway, C.S., Petronis, M., and Rosales, M., 2009, New insights into emplacement mechanisms and geotectonic context for sandstone dikes hosted by Proterozoic granite, Front Range, Colorado: Denver, Colorado, American Association of Petroleum Geologists annual convention. (http://www.searchanddiscovery.com/abstracts/html/2009/annual/abstracts/siddoway.htm).

Siddoway, C.S., Freedman, D.J., and Shatford, S., 2013, ARMO reactivation of Cambrian or older structures: Evidence from the southern Front Range in Colorado Springs: Geological Society of America Abstracts with Programs, v. 45, no. 7, paper no. 401-8.

Smith, D.R., Noblett, J., Wobus, R.A., Unruh, D., Douglass, J., Beane, R., Davis, C., Goldman, S., Kay, G., Gustavson, B., Saltoun, B., and Stewart, J., 1999, Petrology and geochemistry of late-stage intrusions of the A-type, mid-Proterozoic Pikes Peak batholith (Central Colorado, USA):

Implications for petrogenetic models: Precambrian Research, v. 98, p. 271–305, doi:10.1016/S0301-9268(99)00049-2.

Sterne, E.J., 2006, Stacked, "Evolved" Triangle Zones along the Southeastern Flank of the Colorado Front Range: The Mountain Geologist, v. 43, p. 65–92.

Stewart, J.H., Gehrels, G.E., Barth, A.P., Link, P.K., Christie-Blick, N., and Wrucke, C.T., 2001, Detrital zircon provenance of Mesoproterozoic to Cambrian arenites in the western United States and northwestern Mexico: Geological Society of America Bulletin, v. 113, no. 10, p. 1343–1356, doi:10.1130/0016-7606(2001)113<1343:DZPOMT>2.0.CO;2.

Surdam, R.C., Jiao, Z.S., and MacGowan, D.B., 1993, Redox reactions involving hydrocarbons and mineral oxidants: A mechanism for significant porosity enhancement in sandstones: The American Association of Petroleum Geologists Bulletin, v. 77, p. 1509–1518.

Suttner, L.J., Langford, R.P., and O'Connell, A.F., 1984, New interpretation of the stratigraphic relationship between the Fountain Formation and its Glen Eyrie Member, *in* Suttner, L.J., ed., Sedimentology of the Fountain Fan–Delta Complex near Manitou Springs and Cañon City, Colorado: Tulsa, Society of Economic Paleontologists and Mineralogists, Field Trip Guidebook, p. 31–61.

Sweet, D.E., and Soreghan, G.S., 2010, Late Paleozoic tectonics and paleogeography of the Ancestral Front Range: Structural, stratigraphic and sedimentological evidence from the Fountain Formation (Manitou Springs, Colorado): Geological Society of America Bulletin, v. 122, p. 575–594, doi:10.1130/B26554.1.

Swift, D.J.P., 1968, Coastal erosion and transgressive stratigraphy: The Journal of Geology, v. 76, p. 444–456, doi:10.1086/627342.

Temple, J., Madole, R., Keller, J., and Martin, D., 2007, Geologic map of the Mount Deception quadrangle, Teller and El Paso Counties, Colorado: Colorado Geological Survey Open-File Report OF-07-7, scale 1:24,000, 1 sheet.

Timmons, J.M., Karlstrom, K.E., Dehler, C.M., Geissman, J.W., and Heizler, M.T., 2001, Proterozoic multistage (ca. 1.01 and 0.8 Ga) extension recorded in the Grand Canyon Supergroup and establishment of northwest and north trending tectonic grains in the southwestern United States: Geological Society of America Bulletin, v. 113, p. 163–180, doi:10.1130/0016-7606(2001)113<0163:PMCAGE>2.0.CO;2.

Tweto, O.L., 1987, Rock units of the Precambrian basement in Colorado: U.S. Geological Survey Professional Paper 1321-A, 54 p.

Unruh, D.M., Snee, L.W., and Foord, E.R., 1995, Age and cooling history of the Pikes Peak batholith and associated pegmatites: Geological Society of America Abstracts with Programs, v. 27, no. 6, p. 468.

van der Pluijm, B.A., Hall, C.M., Vrolijk, P.J., Pevear, D.R., and Covey, M.C., 2001, The dating of shallow faults in the Earth's crust: Nature, v. 412, p. 172–175, doi:10.1038/35084053.

van der Pluijm, B.A., Vrolijk, P.J., Pevear, D.R., Hall, C.M., and Solum, J., 2006, Fault dating in the Canadian Rocky Mountains: Evidence for Late Cretaceous and early Eocene orogenic pulses: Geology, v. 34, p. 837–840, doi:10.1130/G22610.1.

van Loon, A.J., 2008, Could 'Snowball Earth' have left thick glaciomarine deposits?: Gondwana Research, v. 14, p. 73–81, doi:10.1016/j.gr.2007.05.009

Weil, A.B., Geissman, J.W., and van der Voo, R., 2004, Paleomagnetism of the Neoproterozoic Chuar Group, Grand Canyon Supergroup, Arizona: Implications for Laurentia's Neoproterozoic APWP and Rodinia break-up: Precambrian Research, v. 129, p. 71–92, doi:10.1016/j.precamres.2003.09.016.

Weissenburger, K., Milito, S., and Ellis, D., 2010, Geologic folio Red Rock Open Space, Colorado Springs, Colorado: Colorado Springs, Colorado, Old Colorado City Historical Society, 295 p.

Westrop, S.R., 1986, Trilobites of the Upper Cambrian Sunwaptan Stage, southern Canadian Rocky Mountains, Alberta: Palaeontographica Canadiana, v. 3, 179 p.

Manuscript Accepted by the Society 29 July 2013

Printed in the USA